Annales Societatis Geologorum Poloniae (2025), vol. 95: 189–210. https://doi.org/10.14241/asgp.2025.13

MIDDLE–LATE JURASSIC PELAGIC MICROFACIES AND DEPOSITIONAL EVOLUTION AT THE ALPINE TETHYS MARGIN: THE NIEDZICA-PODMAJERZ SECTION, PIENINY KLIPPEN BELT, POLAND

Kamila KASPEREK[1]*, Renata JACH[1], Daniela REHÁKOVÁ[2], Paulina MILANIAK[1] & Hubert WIERZBOWSKI[3]

[1] *Institute of Geological Sciences, Faculty of Geography and Geology, Jagiellonian University, Gronostajowa 3a, 30-387 Kraków, Poland; e-mail: kamila.kasperek@doctoral.uj.edu.pl; renata.jach@uj.edu.pl; paulina.milaniak@op.pl*
[2] *Department of Geology and Palaeontology, Faculty of Natural Sciences, Comenius University, Ilkovičova 6, 842 15 Bratislava; Slovakia, e-mail: daniela.rehakova@uniba.sk*
[3] *Polish Geological Institute - National Research Institute, Rakowiecka 4, 00-975 Warsaw, Poland; hubert.wierzbowski@pgi.gov.pl*
** Corresponding author*

Kasperek, K., Jach, R., Reháková, D., Milaniak, P. & Wierzbowski, H., 2025. Middle–Late Jurassic pelagic microfacies and depositional evolution at the Alpine Tethys margin: The Niedzica-Podmajerz section, Pieniny Klippen Belt, Poland. *Annales Societatis Geologorum Poloniae*, 95: 189–210.

Abstract: Major geological and ecological transformations, linked to the progressive opening of the ocean basins, extensional tectonics, and changes in pelagic sedimentation occurred across the Tethys during the Bajocian–Tithonian interval. This study reconstructs supra-regional palaeoenvironmental changes, based on pelagic deposits from the Niedzica-Podmajerz section of the Pieniny Klippen Belt, representing the Alpine Tethyan domain. An integrated dataset, including carbon isotope stratigraphy, biostratigraphy, microfacies analysis, and $CaCO_3$ content, provides insights into sedimentary evolution along a submarine slope. The succession reflects a long-term deepening trend, beginning with neritic crinoid-dominated deposition, followed by the accumulation of deeper-shelf sediments, rich in *Bositra* sp., juvenile ammonites, and gastropods, and continuing into basinal deposits, characterized by *Globuligerina*, radiolarian, and *Saccocoma*-filamentous and *Globochaete*-*Saccocoma* assemblages. This facies evolution parallels global phenomena, such as the transgression at the Middle–Late Jurassic transition, a carbonate production crisis, ocean acidification, climate changes and circulation changes, linked to the opening of the Atlantic-Tethys Seaway. Specific intervals of the studied section were assigned to the Oxfordian (Fibrata Zone), the Kimmeridgian (Parvula Acme, Moluccana, and Borzai zones), and the Lower Tithonian (Pulla Acme, Malmica, and Cieszynica zones), on the basis of calcareous dinoflagellate cyst analysis. These intervals correspond to key $\delta^{13}C$ events: the Late Callovian–earliest Oxfordian and Kimmeridgian positive events and a minor negative shift near the Kimmeridgian-Tithonian boundary.

Key words: Calcareous dinoflagellate cysts, carbon and oxygen isotopes, stratigraphy, radiolarites, nodular limestone facies, submarine ridge-slope system.

Manuscript received 11 August 2025, accepted 18 October 2025

INTRODUCTION

The Middle to Late Jurassic period in the Tethyan realm was marked by a significant perturbation in carbonate production, commonly referred to as the carbonate production crisis (cf. Bartolini *et al*., 1996; Cecca *et al*., 2005; Rais *et al*., 2007). Although widely recognized, its expression varied across different basins, reflecting the influence of local tectonics and environmental factors, such as basin bathymetry and the position of depositional settings, relative to the aragonite and calcite compensation depths. In many basins, this disruption was associated with a decline in coral-reef growth, enhanced biosiliceous sedimentation, and reduced carbonate accumulation (Ogg *et al*., 1983; Bartolini and Cecca, 1999; Leinfelder *et al*., 2002; Erba and Tremolada, 2004; Ramajo and Aurell, 2008). These

spatially heterogeneous responses highlight the importance of local- and basin-scale studies, aimed at understanding sedimentary patterns during this time.

In this context, the Pieniny Klippen Belt (PKB) of the eastern Alpine Tethys represents a key area for reconstructing sedimentary evolution across a complex, bathymetrically differentiated setting. The PKB succession includes a range of depositional environments, from submarine-ridge through transitional-slope zones to adjacent deep basins, hosting both carbonate and biosiliceous facies. Of particular importance is the Niedzica Succession and its stratotype, the Niedzica-Podmajerz section, which occupied an intermediate position along the slope between the elevated Czorsztyn Ridge and deeper basinal settings during the Bajocian–Tithonian. The succession captures a long-term deepening trend and a shift in dominant sedimentary regimes, offering a valuable record of palaeoenvironmental changes, linked to regional and supra-regional oceanographic processes.

Whereas the Bajocian–Bathonian interval of the Niedzica-Podmajerz section is well constrained biostratigraphically and chemostratigraphically, the overlying Callovian–Lower Tithonian interval remains comparatively poorly resolved. Nevertheless, this section preserves a valuable record of facies transitions from shallow-marine to basinal settings, making it an important archive for reconstructing palaeoenvironmental change during this understudied interval.

This study aims to reconstruct the palaeoenvironmental evolution, recorded in the Niedzica-Podmajerz section, through an integrated stratigraphic and sedimentological approach. Specifically, the research (1) refines the stratigraphic framework, using new biostratigraphic data from calcareous dinoflagellate cysts in conjunction with high-resolution $\delta^{13}C$ chemostratigraphy of bulk carbonates, focusing on the poorly constrained Upper Callovian to Tithonian interval; (2) evaluates the applicability of $\delta^{13}C$ and $\delta^{18}O$ values as a chemostratigraphic tool in radiolarite-dominated pelagic slope deposits with low carbonate content; (3) correlates the Niedzica $\delta^{13}C$ record with successions in the Tatra Mountains to improve regional stratigraphic resolution; and (4) integrates microfacies analysis to better understand sedimentary processes and palaeoenvironmental trends within this bathymetrically differentiated segment of the Alpine Tethys realm.

GEOLOGICAL SETTING

The PKB is a narrow tectonic zone, located between the Inner Carpathians to the south and the Outer Carpathians to the north, extending over approximately 600 km in a west-east direction, with its width varying from several tens of metres to a few kilometres (Birkenmajer, 1986). This complex structural domain preserves a deformed sedimentary succession of the Alpine Tethys Ocean, developed along its passive margin.

From the Early Jurassic to the Late Cretaceous, the Pieniny Basin formed a part of the Alpine Tethys realm (Fig. 1), characterized by strong bathymetric differentiation and the presence of submarine highs and intervening basins (horst-and-graben architecture; Birkenmajer, 1977). One of the key structural features in this system was the Czorsztyn Ridge, a prominent intrabasinal elevation that significantly influenced sedimentation patterns and facies zonation. The Niedzica-Podmajerz section belongs to the Niedzica Succession, representing a transitional facies zone, deposited on the southeastern slope of the Czorsztyn Ridge (Birkenmajer, 1977; Krobicki and Wierzbowski, 2009; Wierzbowski *et al*., 2021). Sediments of this unit were deposited between the elevated Czorsztyn Ridge, characterized by deposition of crinoidal and nodular limestones, and deeper

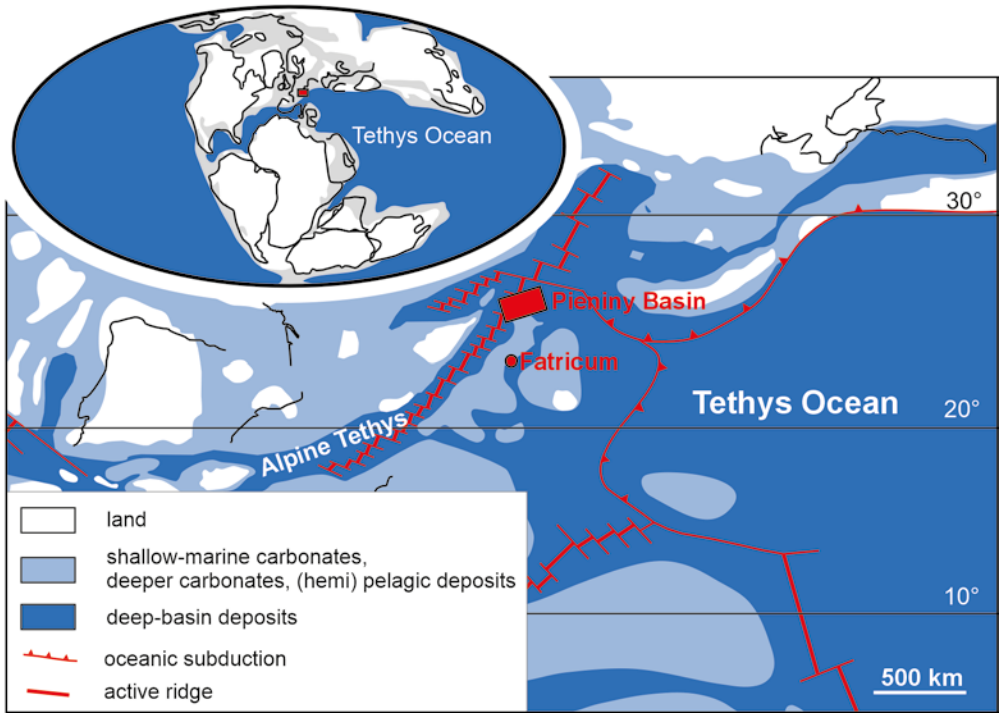

Fig. 1. General palaeogeographic position of the Pieniny Basin during the Middle Callovian (after Thierry and Barrier, 2000; simplified).

settings of the northern Branisko to Czertezik-type succession, characterized by deposition of spotted limestones and radiolarites during the Bajocian–earliest Kimmeridgian (Wierzbowski *et al*., 2021).

NIEDZICA-PODMAJERZ SECTION DESCRIPTION

The Niedzica-Podmajerz section (49°24′50.9″N, 20°17′57.0″E) is located approximately 600 m northwest of the centre of Niedzica village, within the central part of the PKB. The outcrop is exposed in a tectonic window (Birkenmajer and Znosko, 1955), where strata are tilted northward and preserved in an inverted position (Fig. 2). The studied section provides a nearly continuous sedimentary record, spanning the Middle to Upper Jurassic, documenting a gradual transition from neritic crinoidal limestones, through lower nodular limestones, to radiolarites and upper nodular limestones of distinctly pelagic character (Fig. 3). The exposed ca. 32-m-thick succession spans the Bajocian to Lower Tithonian interval and is subdivided into five principal facies (Birkenmajer, 1977; Figs 3, 4A–F, 5). The exposed succession begins with (1) grey crinoidal limestones of the Smolegowa Limestone Formation, overlain by (2) red crinoidal limestones of the Krupianka Limestone Formation. These are followed by (3) lower nodular limestones of the Niedzica Limestone Formation. Above this interval, (4) variegated radiolarites of the Czajakowa Radiolarite Formation are developed, subdivided into the Kamionka, Podmajerz, and Buwałd Radiolarite members, corresponding respectively to the lower red, green, and upper red radiolarites (Birkenmajer, 1977). The succession is overlain by (5) upper nodular limestones of the Czorsztyn Limestone Formation.

The stratigraphy of the Niedzica-Podmajerz section has been relatively well-studied, particularly in the crinoidal and lower nodular limestones, with comprehensive analyses focusing on ammonite biostratigraphy, chemostratigraphy and microfacies (Wierzbowski *et al*., 1999; Krobicki and Wierzbowski, 2004; Krobicki *et al*., 2006b; Arabas, 2016).

Initial age assignments for the lower nodular limestones were proposed by Birkenmajer and Myczyński (1984), who, on the basis of ammonite assemblages, dated these deposits as Upper Bajocian–Callovian. This interpretation was later refined by Wierzbowski *et al*. (1999), who, also using ammonite biostratigraphy, subdivided the sequence more precisely: the lower part was assigned to the uppermost Bajocian, the middle part to the Lower Bathonian, and the upper part tentatively to the Upper Callovian–Oxfordian.

Further constraints on the age of overlying radiolarites were provided by radiolarian data. According to Widz (1991) and Birkenmajer and Widz (1995), the green and upper red radiolarites correspond to the Middle–Upper Oxfordian to Lower Kimmeridgian interval (UAZ 9–10). It is worth noting that the section at Czajakowa Skała klippe, the stratotype of the Czajakowa Radiolarite Formation, was also examined by these authors. On the basis of material, collected exclusively from the lower red radiolarites, they identified assemblages corresponding to the Middle Callovian to Middle–Upper Oxfordian (UAZ 8–9).

On the basis of the calcareous dinoflagellata cysts, the upper nodular limestones of Czorsztyn Limestone Formation in the Niedzica-Podmajerz section was assigned to the uppermost Kimmeridgian Borzai Zone and the Lower Tithonian Malmica and Cieszynica zones (Nowak, 1973, 1976). Subsequent biostratigraphic studies of calcareous dinoflagellate cysts, conducted in the Niedzica Succession by Ławrynowicz (2000), confirmed the age and zonal assignments, proposed by Nowak. A comprehensive biostratigraphy synthesis from the Bajocian to the Tithonian in the Niedzica-Podmajerz section was presented by Krobicki *et al*. (2006a). More recently, Arabas (2016) integrated

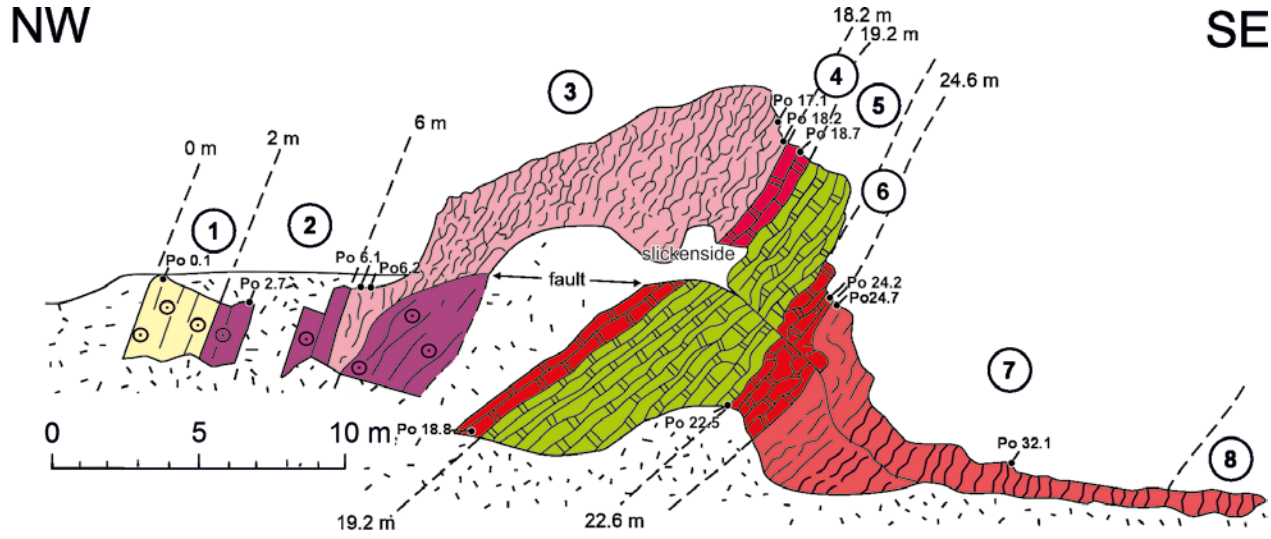

Fig. 2. Geological section of the Niedzica-Podmajerz section, after Birkenmajer and Znosko (1955), modified. Lithological legend: 1. Grey crinoidal limestones of the Smolegowa Limestone Formation, 2. Red crinoidal limestone of the Krupianka Limestone Formation, 3. Lower nodular limestone of the Niedzica Limestone Formation, 4. Lower red radiolarites of the Kamionka Radiolarite Member, 5. Green radiolarites of the Podmajerz Radiolarite Member, 6. Upper red radiolarites of the Buwałd Radiolarite Member, 7. Upper nodular limestone of the Czorsztyn Limestone Formation, 8. Calpionellid limestone of the Dursztyn Limestone Formation.

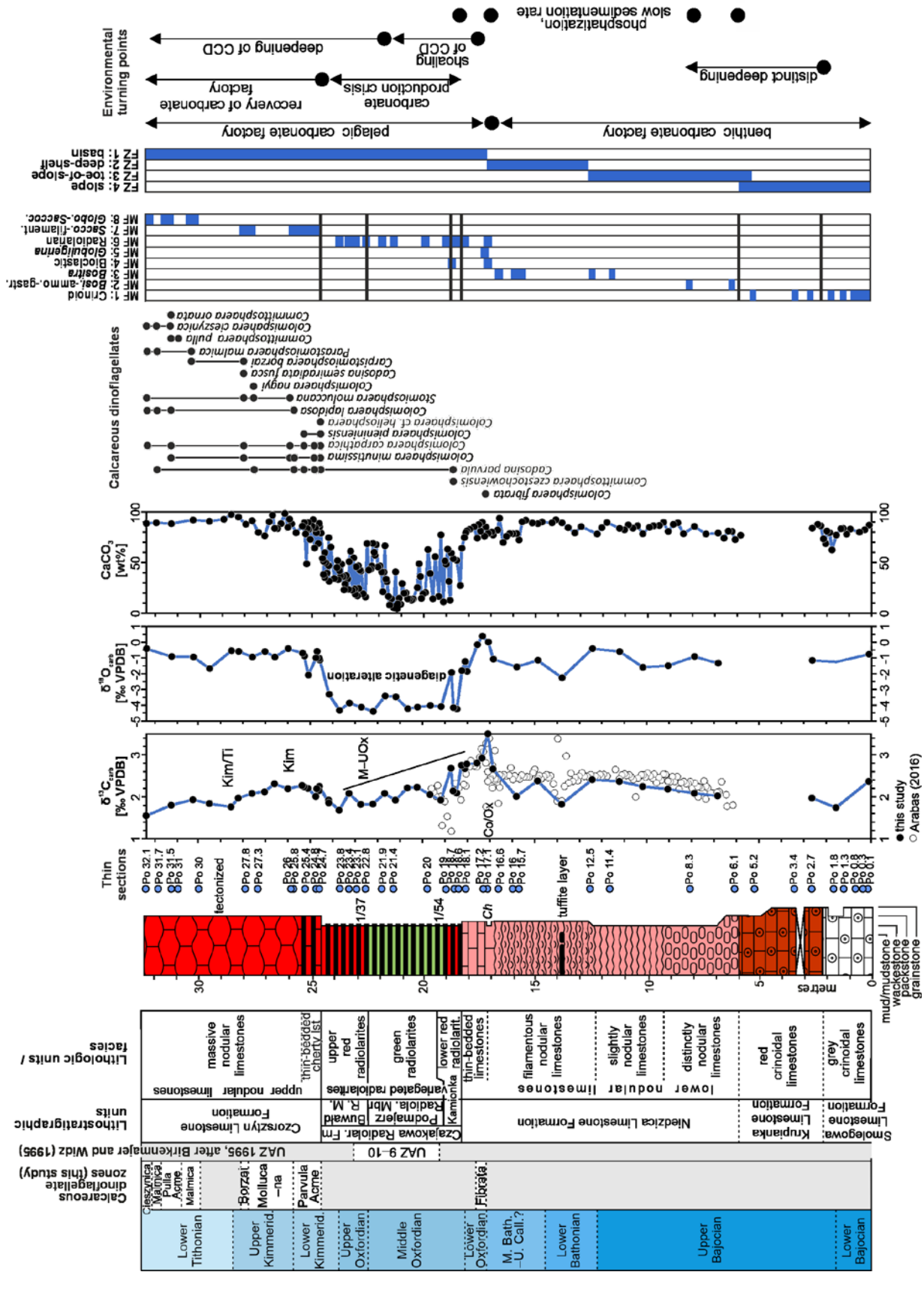

Fig. 3. Bajocian–Lower Tithonian deposits of the Niedzica Succession in the Niedzica-Podmajerz section (Pieniny Klippen Belt): lithology, biostratigraphy, carbon and oxygen isotopes, $CaCO_3$ content, microfacies (MF), and their distribution within facies zones (FZ). Legend: Ch – *Chondrites* isp.; 1/37 and 1/57 – radiolarian samples documented by Widz (1991) and Birkenmajer and Widz (1995). Abbreviations of excursions and boundary events: Co/Ox – Callovian/Oxfordian; M–UOx – Middle–Upper Oxfordian; Kim – Kimmeridgian; Kim/Ti – Kimmeridgian/Tithonian.

Fig. 4. Details of the Niedzica-Podmajerz outcrop with sample locations and key lithological boundaries, corresponding to the lithostratigraphic section in Figure 3. **A.** Grey and red crinoidal limestones (0–2.5 m in the section). **B.** Red crinoidal limestones and lower nodular limestones (5.5–7.0 m). **C.** Lower nodular limestones (7.5–9.0 m). **D.** Lower red and green radiolarites (18.9–19.6 m). **E.** Upper red and green radiolarites (21.6–23.0 m). **F.** Upper nodular limestones (25.7–26.3 m).

chemostratigraphic data and identified, in the uppermost part of the lower nodular limestones, the global positive $\delta^{13}C$ excursion, correlated with the Upper Callovian–Middle Oxfordian interval. In contrast to the lower part of the section, the upper succession has not yet been studied in terms of its stable isotope composition.

MATERIAL, METHODS AND TERMINOLOGY

The section was studied bed-by-bed with detailed sampling, for microfacies analysis, carbonate content, and integrated stratigraphy, primarily on the basis of the results of the M.Sc. thesis by Milaniak (2021). A total of 41 thin sections was examined, using a LEICA DM 2500 polarizing microscope at the Department of Geology and Palaeontology, Faculty of Natural Sciences, Comenius University in Bratislava. Microfacies and biogenic components were documented with an Axiocam ERc 5s digital camera. The rock samples and the thin sections are stored at the Institute of Geological Sciences, the Jagiellonian University in Kraków.

The microfacies of both carbonate and siliceous sediments were classified according to Dunham's (1962) scheme. Standard microfacies types (MF) and facies zones (FZs) were determined following the schemes of Wilson (1975) and

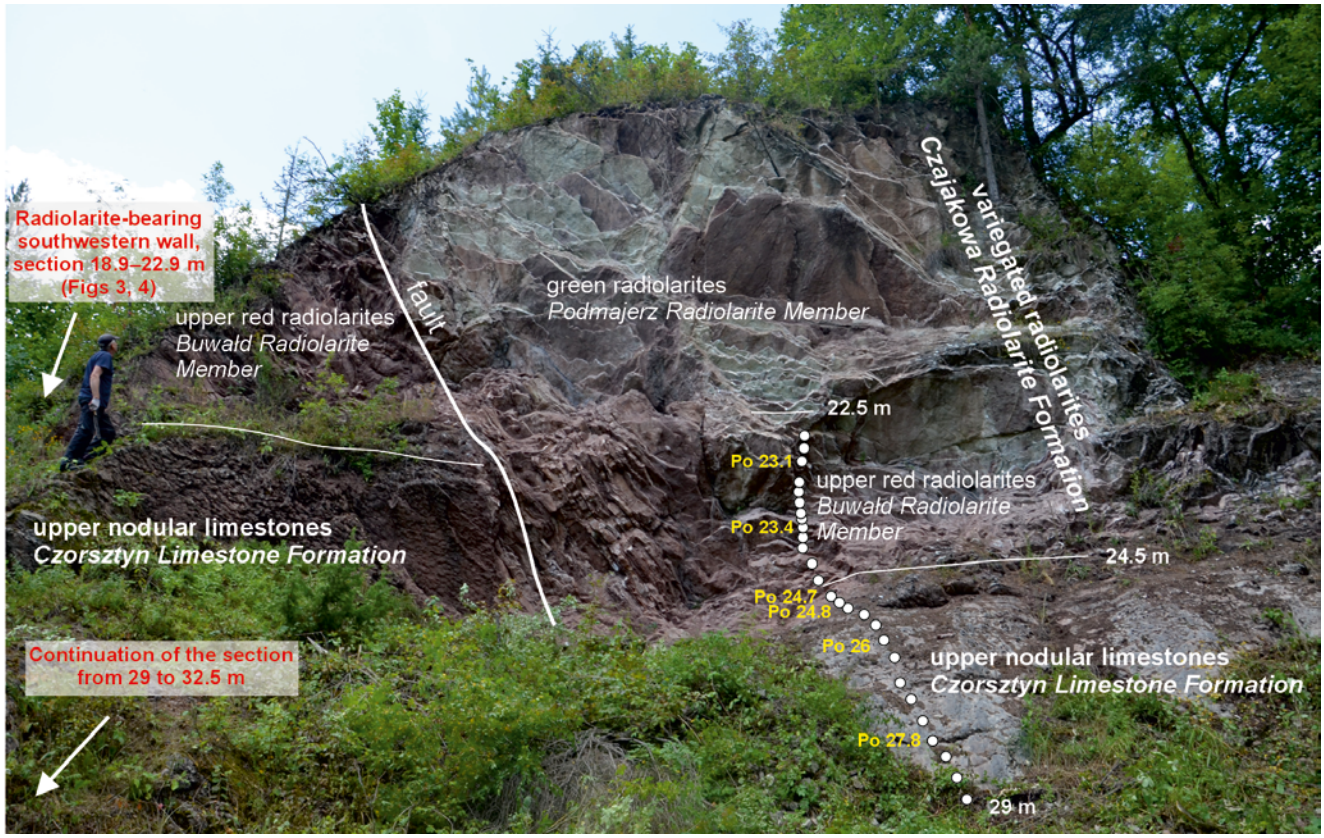

Fig. 5. General field view of the southeastern wall of the Niedzica-Podmajerz section. The cliff is composed predominantly of radiolarites, with nodular limestones exposed at its base. Sample locations are indicated in Figure 3.

Flügel (2004) but applied here in a modified form. The calcareous dinoflagellate zonation applied in this study follows Lakova *et al*. (1999, 2007) and Reháková (2000a, b).

In the studied material, the term *Bositra* sp. is applied only to thin-shelled bivalve remains from the Bajocian to Early Oxfordian, reflecting the stratigraphic range of *Bositra buchi*. For younger deposits, the more general term "filaments" is used, due to the uncertainty in precise taxonomic identification of Late Jurassic forms. This terminological issue was discussed in detail by Tomašových *et al*. (2020), who provide the most comprehensive overview of the problem.

Stable isotope compositions ($\delta^{13}C$ and $\delta^{18}O$ values) of 51 bulk sediment samples were analysed in the Stable Isotope Laboratory of the GeoZentrum Nordbayern in Erlangen, Germany. Carbonate powders reacted with 100% phosphoric acid at 70 °C, using a Gasbench II connected to a ThermoFisher Delta V Plus mass spectrometer. All values are reported in per mil, relative to V-PDB. Reproducibility and accuracy were monitored by replicate analysis of laboratory standards, calibrated by assigning a $\delta^{13}C$ of +1.92‰ to NBS19 and a $\delta^{18}O$ of -2.21‰ to NBS19. The reproducibility and accuracy of the measurements was monitored, over the course of analyses, by replicate analysis of laboratory standards Sol 2 (n = 10) and Erl-5 (n = 9). Reproducibility for $\delta^{13}C$ and $\delta^{18}O$ values was 0.04‰ and 0.05‰ (±1σ S.D.) for Sol 2, and 0.05‰ and 0.04‰ (±1σ S.D.) for Erl-5, respectively.

The analyses of calcium carbonate content were carried out on 207 samples. Analyses were performed with an Eijkelkamp calcimeter, which operates in accordance with the Scheibler method. The repeatability of measurements was better than 0.6% $CaCO_3$, based on replicate measurements of homogenized samples.

RESULTS

Facies and microfacies description

Five principal facies have been distinguished in the carbonate-siliceous succession (Bajocian–Lower Tithonian) of the Niedzica-Podmajerz section (Birkenmajer and Znosko, 1955; Birkenmajer, 1977; Wierzbowski *et al*., 1999; Krobicki *et al*., 2006b). Their classification is based on macroscopic field observations, including sedimentary structures (e.g., bedding style, presence and morphology of nodules) as well as textural attributes, such as component types, their relative abundances, and spatial distribution; sediment colour was also considered as a diagnostic feature.

Grey crinoidal limestones

Facies description: Distinctive grey crinoidal limestones, over 2 m thick, form the lower part of the Niedzica-Podmajerz section and correspond to the Smolegowa Limestone Formation (Figs 3, 4A). The crinoidal limestones are light greyish, or pinkish, fine- to medium-grained, and show a marked dominance of crinoidal debris (Fig. 6A). They are either massive or exhibit poorly developed bedding. Macroscopic observations reveal that the facies contains a notable admixture of fine-sand-sized siliciclastic and yellowish

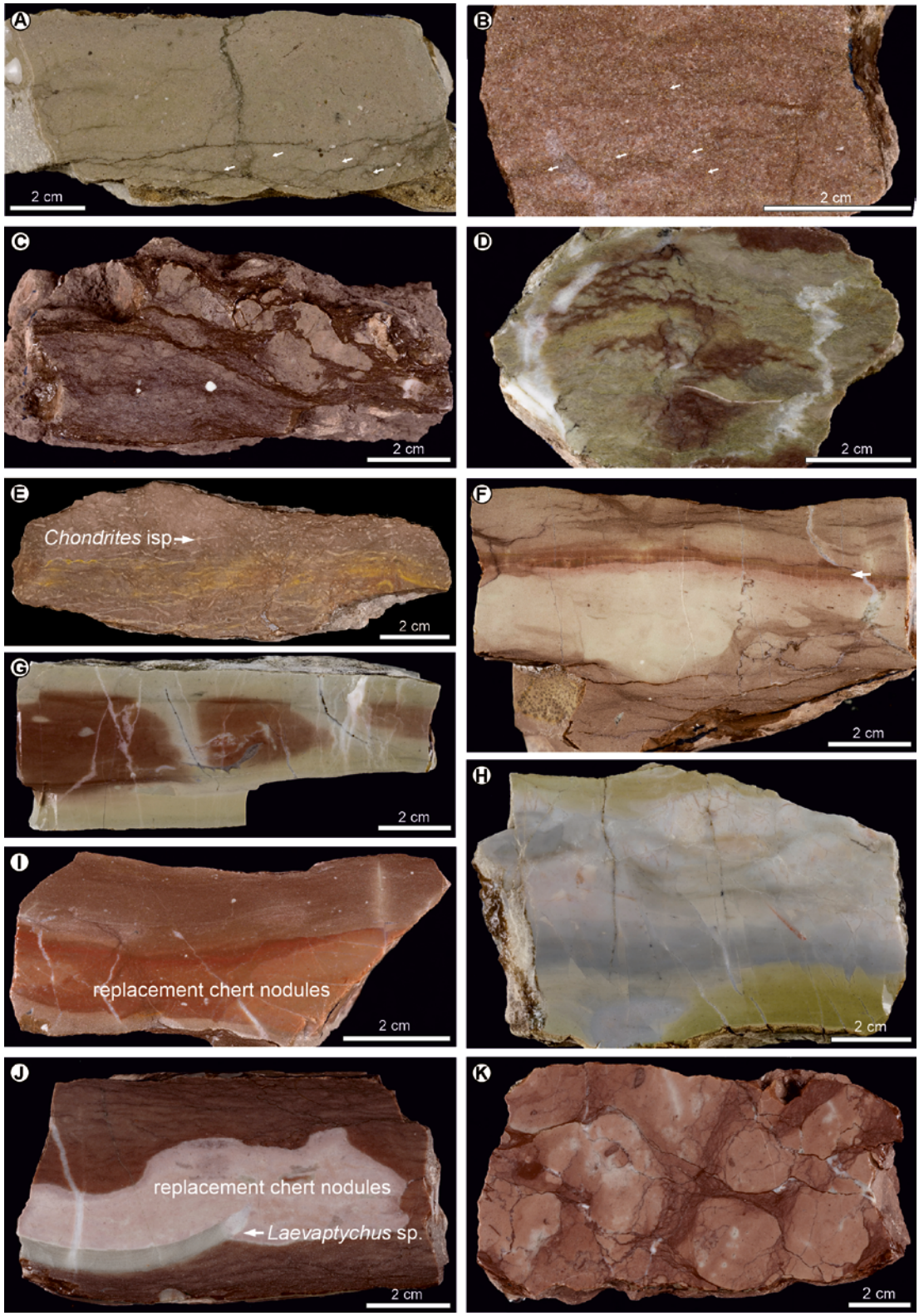

Fig. 6. Main lithologies of the Middle–Upper Jurassic Niedzica-Podmajerz succession of the Pieniny Klippen Belt, polished slab surfaces. For sample locations, see Figure 3. **A.** Light-grey, fine- to medium-grained crinoidal limestone at 0.1 m; white arrows indicate dispersed, fine-sand-sized yellowish dolomite grains. **B.** Red crinoidal limestone at 2.7 m, containing numerous yellow, sand-sized dolomite grains; several individual grains are marked with arrows. **C.** Lower red nodular limestone at 8.6 m, characterized by a prominent nodular fabric with strong contrast between carbonate-rich nodules and more easily weathered marly matrix. **D.** Red bioclastic nodular limestone of the lower nodular limestones at 14.4 m, displaying typical filament-fitted fabric, characteristic of the *Bositra* facies. **E.** Thin-bedded limestone of the lower nodular limestones at 17.1 m, with the numerous trace fossil *Chondrites* isp. **F.** Lower nodular limestone at 18.1 m, showing subtle nodular texture and thin chert intercalations. **G.** Lower red radiolarite at 19 m. **H.** Green radiolarite at 21 m. **I.** Upper red radiolarite at 23.4 m, with irregular replacement chert. **J.** Thin-bedded cherty limestone facies of the upper nodular limestone at 25 m, with irregular replacement chert and a specimen of *Laevaptychus* sp. **K.** Upper nodular limestone at 31 m.

dolomitic clasts (Fig. 6A). Macrofossils, including belemnites, ammonites, and brachiopods, are particularly common in the lowermost part of the facies (Wierzbowski *et al*., 1999; Krobicki *et al*., 2006b). The carbonate content of this facies reaches approximately 79% (Fig. 3). The transition to the overlying red crinoidal limestones is marked by the occurrence of thin marly intercalations (1.7–2 m; Fig. 6A).

Microfacies description: Crinoid packstones to grainstones (microfacies MF 1; Figs 3, 7A) represent the dominant microfacies within this facies, with sorting becoming progressively poorer towards the top. Redeposited crinoid ossicles, including columnals, brachials, cirrals, and rare pluricolumnals, constitute the principal skeletal component throughout this facies. These are accompanied by peloids, subordinate fragments of ostracods, bryozoan fragments, echinoids and ophiurids, while bivalve shells occur only sporadically. The benthic foraminiferal assemblage is dominated by miliolids and textulariids: *Ophthalmidium* sp., *Gaudryina* sp., *Ammobaculites* sp., *Meandrospira* sp., and *Glomospira* sp., with less abundant calcite-walled forms, such as *Lenticulina* sp., *Nodosaria* sp., *Spirillina* sp., and *Frondicularia* sp. Calcareous dinoflagellate cysts (*Cadosina* sp., *Colomisphaera* sp.) occur though they are rare.

Siliciclastic admixtures, visible under the microscope, are composed predominantly of silt- to fine sand-sized quartz grains, dolomites, dedolomites, and micritic lithoclasts. The components are typically cemented by syntaxial calcite overgrowths, developed on echinoderm fragments. Locally, bioturbation of the micritic matrix led to the concentration of calcified sponge spicules, which often form nest-like concentrations within the sediment. These zones, also show frequent Fe-hydroxide-impregnated stylolites and dissolution seams, which highlight the boundaries of bioclasts and suggest advanced pressure-solution diagenesis. Some bioclasts, particularly crinoid and bivalve fragments, display signs of silicification.

Red crinoidal limestones

Facies description: This facies forms a ~4 m thick unit (2–6 m; Fig. 3) in the Niedzica-Podmajerz section and is assigned to the Krupianka Limestone Formation. Distinctly bedded limestone displays a reddish to brownish colour, with occasional greenish hues (Fig. 4A). Macroscopically, the rock is composed of fine- and medium-grained crinoid fragments, with columnals typically <0.5 mm in diameter (Fig. 6B). Macrofossils are rare and poorly preserved, but

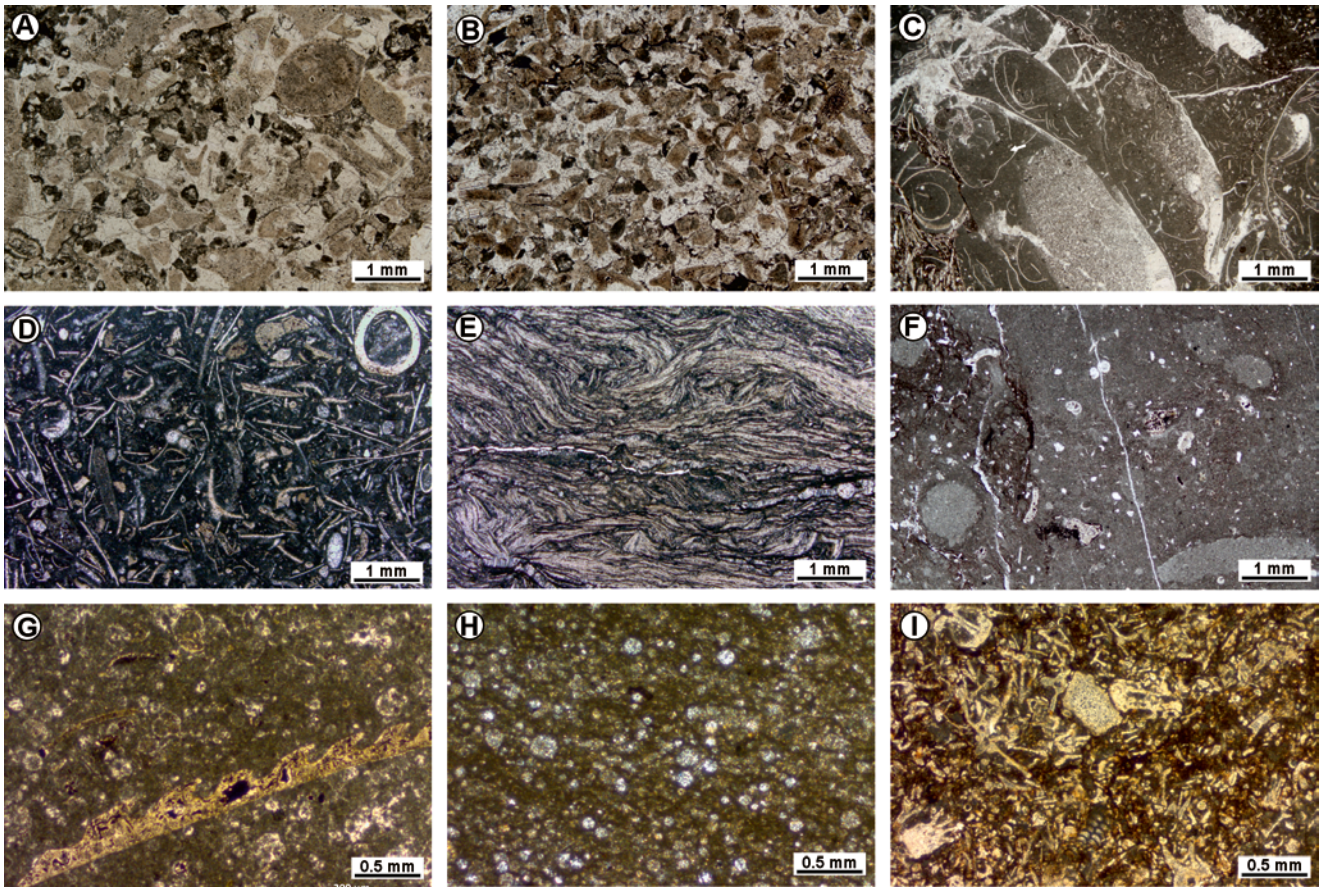

Fig. 7. Microfacies of the Niedzica-Podmajerz section. For sample locations, see Figure 3. **A.** Medium-grained crinoidal grainstone with syntaxial cement and common admixture of sand-sized siliciclastic and dolomite grains; grey crinoidal limestone at 0.8 m. **B.** Fine-grained crinoidal grainstone with abundant yellowish dolomite, dedolomite and quartz clasts; red crinoidal limestone at 2.7 m. **C.** *Bositra*-juvenile ammonites-gastropods wackestone; lower nodular limestone at 8.3 m. **D.** *Bositra* wackestone to packstone with spores of *Globochaete alpina* Lombard; lower nodular limestone at 15.7 m. **E.** *Bositra* packstone with densely packed filaments; lower nodular limestone at 16.6 m. **F.** Intensely bioturbated bioclastic wackestone with trace fossils of *Chondrites* isp., visible as light spots against a darker. **G.** *Globuligerina* wackestone with intensely bored aptychi; lower nodular limestone at 17.2 m. **H.** Radiolarian packstone with radiolarians filled with chalcedony; lower red radiolarite at 18.6 m. **I.** *Saccocoma*-filamentous packstone; upper nodular limestone at 31.5 m.

include ammonites, belemnites, and brachiopods (Birkenmajer and Znosko, 1955; Krobicki *et al*., 2006b). The $CaCO_3$ content averages ~81% (Fig. 3). The facies contains frequent, yellowish, sand-sized dolomitic and dedolomitic clasts, along with scattered siliciclastic grains. Glauconite grains are present only sporadically.

The transition between the red crinoidal limestones and the overlying lower nodular limestones is gradual and somewhat arbitrary (Fig. 4B). A subtle nodular character appears in the uppermost beds of the former, while the lowermost beds of the latter still contain crinoidal debris, indicating facies overlap.

Microfacies description:The dominant microfacies are crinoid packstones to grainstones (MF 1; Figs 3, 7B), composed primarily of densely packed crinoid ossicles (columnals, brachials and cirrals), accompanied by subordinate peloids, fragments of echinoids, ophiuroids, sponge spicules, and bivalves, less frequent to rare foraminifers (*Spirillina* sp., *Lenticulina* sp., *Nodosaria* sp., *Frondicularia* sp.), miliolid foraminifera, ostracods, and bryozoans. The uppermost part of the facies is characterized by the first occurrence of juvenile ammonites and thin-shelled bivalves, most probably of the genus *Bositra* (see the explanation of terminology in the section Material, Methods, and Terminology). Bioclasts are locally silicified, and some display evidence of borings. Syntaxial calcite cement predominates around echinoderm fragments, while a micritic matrix occurs more commonly in bioturbated or poorly sorted sediment. Siliciclastic admixtures are dominated by sand-sized micritic carbonate grains and silty quartz, with rare occurrences of glauconite.

Stylolites are frequent throughout the unit, often associated with insoluble residues, enriched in Fe-hydroxides and terrigenous components. Crinoid fragments commonly exhibit iron staining, increasing toward the top of the unit.

Lower nodular limestones

Facies description: The lower nodular limestones, occurring above the red crinoidal limestones and below the variegated radiolarites in the Niedzica-Podmajerz section, are dark red, partly marly, and are assigned to the Niedzica Limestone Formation, corresponding to Rosso Ammonitico-type facies. The average carbonate content is approximately 83% (Fig. 3). In vertical section, this facies shows marked variability in the degree of nodularity.

The lower interval (6–9.2 m) is composed mainly of distinctly nodular limestones, with pinkish and greenish nodules (1–3 cm in diameter), embedded in a dark red, marly–ferruginous matrix (Fig. 6C). The nodules are loosely packed and easily separable, and the sediment is intensely bioturbated. Macrofossils include abundant crinoid fragments, bivalves, ammonites, nautiloids, brachiopods, aptychi, belemnites, and gastropods.

The middle interval (9.2–17 m) retains the nodular structure, but it becomes progressively more diffuse, with less distinct nodule boundaries (Figs 4C, 6D). Around 14 m, a discontinuous tuffite layer of dark-green colouration occurs (Fig. 3).

The upper interval (17–18.2 m) is composed of thin-bedded limestones. At its base, an 8-cm-thick red micritic limestone bed exhibits a bioturbated fabric with the clearly visible trace fossil *Chondrites* isp. (Fig. 6E; sample Po 17.1). Higher in the section (17.6–18.2 m), the succession is dominated by red limestones with faint nodular textures and thin radiolarian chert interbeds (Fig. 6F). The boundary between the lower nodular limestones and the overlying radiolarites is defined by the onset of a marked increase in SiO_2 content, corresponding to the first bed exceeding 50% (Fig. 3).

Microfacies description: The interval between 6 and 9.2 m represents a *Bositra*-juvenile ammonite-gastropod microfacies (wackestone and packstone; MF 2; Figs 3, 7C), rich in *Bositra* sp. and juvenile ammonites, with common gastropods and less frequent crinoid ossicles. Additional components include sponge spicules of rhax type, ostracods, bivalves, spores of *Globochaete alpina* Lombard, planktonic protoglobigerinid foraminifera *Globuligerina oxfordiana* (Grigelis), and calcite-walled foraminifera, such as *Lenticulina* sp., *Spirillina* sp., *Nodosaria* sp., *Miliospirella* sp., and *Rumanolina feifeli seiboldi* (Lutze). Bioclasts at the base of this unit are intensely bored, with many exhibiting signs of phosphatization (samples Po 6.1 and Po 8.3).

MF 3 is represented by *Bositra* microfacies, occurring between 9.2–17 m in the section (Figs 3, 7D, E). *Bositra* sp., some with unusually large shells, are abundant, often mixed with *Globochaete alpina*, juvenile ammonites, crinoid ossicles, sponge spicules of the rhax type, ostracods, gastropods, bivalves (with marks of borings), calcite-walled foraminifera, including *Lenticulina* sp., *Spirillina* sp., *Spirillina andreae* Bielecka, *Nodosaria* sp., planktonic foraminifera *Globuligerina oxfordiana*, benthic species *Compactogerina stellapolaris* (Grigelis), *Andersenolina delphinensis* (Arnaud-Vanneau, Boisseau, Darsac), *Rumanolina feifeli feifeli* (Paalzow), and miliolids – *Ophthalmidium* sp., *Ophthalmidium pseudocarinatum* (Dain), and *Miliospirella* sp. Up-section, the texture gradually changes from wackestone to packstone.

MF 4 (at 17.1 m, sample Po 17.1) consists of a burrowed bioclastic to radiolarian wackestone (Figs 3, 7F). The limestone is intensely stylolitized and fractured, containing fragments of crinoids, echinoids, bivalves (with borings), ophiuroids, planktonic foraminifera *Globuligerina* sp., calcified radiolarians, and abundant cysts of *Colomisphaera fibrata* (Nagy) (Fig. 8A). The benthic foraminiferal assemblage includes calcite-walled and miliolid foraminifera (*Lenticulina* sp., *Spirillina* sp., *Frondicularia* sp., *Miliospirella* sp., *Nodosaria* sp., *Rumanolina* sp., *Andersenolina* sp.). Rare fragments of *Saccocoma* sp. are also present. The matrix is slightly recrystallized, with abundant silty quartz, scattered dolomitic clasts and rare spheroidal grains, interpreted as microbial stromatolite clasts, likely representing unattached, reworked microbial oncoids or microstromatolites. Some of bioclasts are phosphatized.

MF 5 (at 17.2 m, sample Po 17.2) contains recrystallized *Globuligerina* wackestone to packstone (Fig. 7G), with juvenile ammonites (some showing geopetal structures), ostracods, crinoids, aptychi, rhyncholites, and bivalve shells (locally with borings). The deposit includes scarce dolomitic clasts and reworked biomicrite limestone fragments, containing planktonic foraminifera and *Bositra* sp. Some bioclasts are impregnated with pyrite and Fe-hydroxides, and the matrix contains dispersed organic matter.

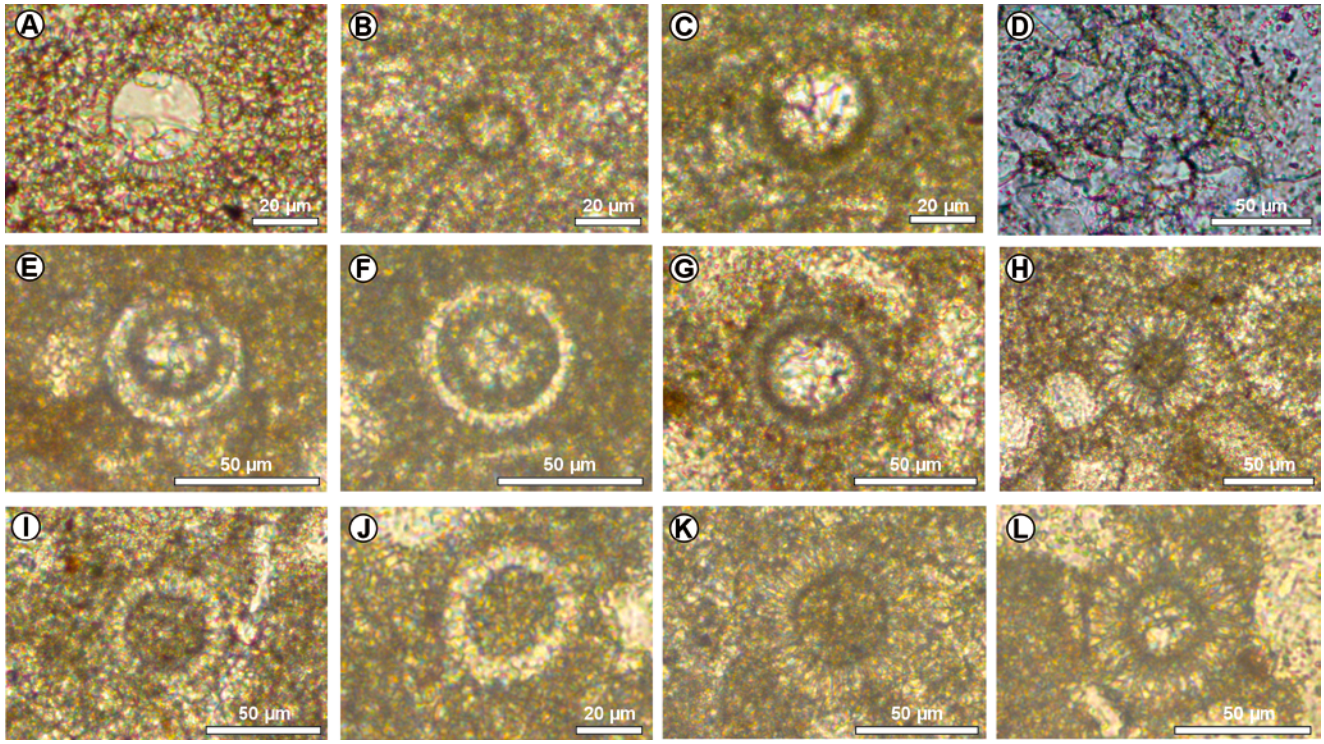

Fig. 8. Oxfordian–Lower Tithonian calcareous dinoflagellates. For sample locations, see Figure 3. **A.** *Colomisphaera fibrata* Nagy, sample at 17.1 m; **B.** *Cadosina parvula*, sample at 18.7 m; **C.** *Committosphaera czestochowiensis*, sample at 18.7 m; **D.** *Stomiosphaera moluccana*, sample at 27.8 m; **E.** *Carpistomiosphaera borzai*, sample at 30 m; **F.** *Parastomiosphaera malmica*, sample at 30 m; **G.** *Committosphaera pulla*, sample at 31 m; **H.** *Committosphaera ornata*, sample at 31 m; **I.** *Colomisphaera minutissima*, sample at 31 m. **J.** *Colomisphaera lapidosa*, sample at 32.1 m; **K.** *Colomisphaera carpathica*, sample at 32.1 m; **L.** *Colomisphaera cieszynica*, sample at 32.1 m.

MF 6 (at 18.1 m) consists of laminated radiolarian wackestone and packstone. Radiolarian tests are variably preserved, as siliceous or calcified tests within a microcrystalline silica and chalcedony matrix. The facies contains sponge spicules, *Bositra* sp., ostracods, globochaetes, rare *Saccocoma* sp., and benthic foraminifera (*Spirillina* sp., *Nodosaria* sp.). The matrix is stylolitized, cut by calcite veins, and locally impregnated with iron hydroxides.

Radiolarites

Facies description: The uppermost part of the Niedzica-Podmajerz section (18.2–24.7 m; Figs 3, 4D, E, 5) comprises ~7-m-thick variegated radiolarites (Czajakowa Radiolarite Formation). Beds are typically 5–10 cm thick, with no visible trace fossils. Shale interbeds are very thin and poorly developed. Variegated radiolarites are subdivided into three lithostratigraphic units: (1) Lower red radiolarites (18.2–19.2 m), 1 m thick, are composed of calcareous, red to greenish red radiolarites (Fig. 6G). The average carbonate content is approximately 43%; however, this facies exhibits marked fluctuations in $CaCO_3$ content, ranging from 11% to 63%. (2) Green radiolarites (19.2–22.5 m) are 3.26 m thick (Fig. 6H). The average carbonate content is approximately 33%, with distinct fluctuations, ranging from consistently low values (as low as 5%) to markedly higher concentrations (up to 68%) in the upper part of the green radiolarites. (3) Upper red radiolarites (22.5–24.6 m; Fig. 6I). 2 m thick, comprise red radiolarites, intercalated with red replacement-chert layers. The average carbonate content is approximately 40%; however, within the upper red radiolarites, a consistent increase in $CaCO_3$ content is observed, ranging from 16% to 54%.

Microfacies description: Radiolarites are dominated by radiolarian wackestones and packstones (MF 6; Fig. 7H). Radiolarian tests and sponge spicules are commonly recrystallized and filled with chalcedony or microcrystalline quartz. In this facies, replacement cherts are widespread, forming either diffuse or well-defined chert layers. Accessory components, occurring mainly in the lower and upper red radiolarites, include aptychi, with silicified fragments of *Laevaptychus* sp., filaments, crinoid fragments, bivalves, and, in some samples, globochaetes. Rare fragments of *Saccocoma* sp. (sample Po 21.4) and benthic foraminifera (*Spirillina* sp., *Lenticulina* sp., *Nodosaria* sp.) are also present.

Notably, cysts of *Cadosina parvula* (Wanner) (Fig. 8B) and *Committosphaera czestochowiensis* Řehánek (Fig. 8C) were identified in biomicrite layers of lower red radiolarite (Fig. 3; sample Po 18.7). In the same sample, several bioclasts exhibit evidence of phosphatization.

Several microfacies show subtle lamination and, less commonly, normal grading, as well as stylolitization and microfractures, filled with bladed calcite. Locally, scattered organic matter is concentrated within several thin laminae.

Upper red nodular limestones

Facies description: The uppermost part of the Niedzica-Podmajerz section (24.6–32.5 m) consists of a 12-m-thick succession of upper nodular limestones (Czorsztyn Limestone

Formation), of which only the lower 8 m were examined in this study. Compared to the lower nodular limestones, these beds are more massive, lighter in colour, and have a slightly higher carbonate content (~84%; Fig. 3).

The lower part of this unit (24.6–25.8 m) comprises reddish, thin-bedded cherty limestones of Rosso ad Aptichi-type facies. Irregular replacement cherts and specimens of *Laevaptychus* sp. occur in this interval (Fig. 6J). Up-section (25.6–32.5 m), the nodular fabric becomes progressively more pronounced, culminating in typical Rosso Ammonitico-type facies. These are characterized by closely packed, carbonate-rich spheroidal to elongate nodules, separated by an intensely red matrix with abundant dissolution seams, impregnated with Fe-hydroxides and numerous stylolites (Fig. 6K). The texture most likely reflects early diagenetic cementation and compaction, which produced subtle internal differentiation within the sediment, later accentuated by selective weathering. It is noteworthy that on a well-weathered upper bedding surface of one of the beds, the nodules exhibit a distinct preferred orientation. Following the concept of a "pseudonodular" texture, proposed by Martire (1996) for the Rosso Ammonitico facies, these limestones can be regarded as pseudonodular, a term also used by earlier authors (e.g., Birkenmajer, 1977).

Microfacies description: The upper nodular limestones (24.6–32.5 m) of the Czorsztyn Limestone Formation are composed mainly of *Saccocoma*-filamentous packstones (MF 7; 24.6–28 m) and *Globochaete–Saccocoma* wackestones to packstones (MF 8; 30–32 m; Fig. 7I), locally enriched in radiolarians. The assemblage includes *Saccocoma* sp., filaments, *Globochaete alpina*, calcified radiolarians, crinoid ossicles, ostracods, bivalves, aptychi, juvenile ammonites, echinoid spines, ophiuroids, and benthic foraminifera (*Spirillina* sp., *Lenticulina* sp., *Gaudryina* sp., *Textularia* sp.), accompanied by diverse calcareous dinoflagellate cysts (Fig. 8D–L), such as: *Stomiosphaera moluccana* (Wanner), *Carpistomiosphaera borzai* (Řehánek), *Cadosina parvula* Nagy, *Parastomiosphaera malmica* (Borza), *Committosphaera pulla* (Borza), *Committosphaera ornata* (Nowak), *Colomisphaera minutissima* (Nowak), *Col. lapidosa* (Nowak), *Col. carpathica* (Borza), *Col. cieszynica* (Řehánek), *Col.* cf. *heliosphaera* (Vogler), *Col. pieniniensis* (Řehánek), *Cadosina semiradiata fusca* (Wanner) and *Col. nagyi* (Borza).

Calcareous dinoflagellate cyst biostratigraphy

The biostratigraphic framework of the Oxfordian to Lower Tithonian deposits investigated is established on the basis of calcareous dinoflagellate cysts. On the basis of the microfacies context and taxonomic composition, the zonation was refined into seven distinct zones (Fig. 3). The calcareous dinoflagellate cysts are generally well preserved, even in samples with a recrystallized matrix. It can therefore be assumed that their surface was protected by an organic coating.

Fibrata Zone

The oldest calcareous dinoflagellate cyst zone, recognised in the Niedzica-Podmajerz section, is the Fibrata Zone. It occurs in the lower nodular limestones at 17.2 m, within bioclastic wackestones containing *Chondrites* isp. This level is marked by the first occurrence (FO) of the index species *Colomisphaera fibrata* (Fig. 8A), confirming its assignment to the Fibrata Zone. According to Lakova (1993), this zone ranges from the lowermost Oxfordian to the lower part of the Upper Oxfordian, with the Callovian–Oxfordian boundary situated somewhat below its base. Thus, although the appearance of *C. fibrata* at 17.2 m indicates entry into the Fibrata Zone.

Parvula Acme Zone

The next, younger zone in the section is assigned to the Parvula Acme Zone. It is documented between 24.7 and 25.8 m, within thin-bedded cherty limestones representing a *Saccocoma*–filamentous packstone microfacies, corresponding to the lowermost part of upper nodular limestones. The interval is characterized by a cyst assemblage, dominated by *Cadosina parvula*, the sharp increase in abundance of which defines the base of the Parvula Acme Zone, following the concept of Reháková (2000a). The index species is accompanied by common *Colomisphaera minutissima* and *Col. carpathica*, and rarer occurrences of *Col. lapidosa*, *Col. pieniniensis*, and *Col.* cf. *heliosphaera*. According to Reháková (2000a, b), *C. parvula* became most abundant at the beginning of the Kimmeridgian, and this acme event was used to define the Parvula Acme Zone, which is confined to the Lower Kimmeridgian.

Moluccana Zone

The next cyst assemblage is recorded between 25.9 and 27.5 m, within the lower part of the upper nodular limestones, composed of *Saccocoma*-filamentous packstones. The association is dominated by *Stomiosphaera moluccana*, accompanied by *Colomisphaera carpathica*, *Col. pieniniensis*, *Col. nagyi* and *Col. minutissima*. This association defines the Moluccana Zone of the Upper Kimmeridgian, which correlates with the Acanthicum, Eudoxus, and Beckeri ammonite zones (Reháková, 2000a, b; Reháková *et al*., 2011). According to Reháková (2000a), this zone is defined by the first occurrence (FO) of *Stomiosphaera moluccana* and is also marked by a pronounced increase in *Saccocoma* abundance as well as frequent occurrences of *Globochaete alpina*.

Borzai Zone

A slightly younger zone in the section is assigned to the Borzai Zone. It is documented at 27.9 m, within the upper nodular limestones, representing a *Saccocoma*-filamentous microfacies. The interval is marked by the FO of *Carpistomiosphaera borzai*, which defines the base of the Borzai Zone, following the biostratigraphic concept of Reháková (2000a). Although *C. borzai* is rare in the assemblage, its presence is biostratigraphically significant. The associated phytoplankton includes *Stomiosphaera moluccana* (Fig. 8D), *Colomisphaera carpathica*, *Col. minutissima*, and *Cadosina semiradiata fusca*. This assemblage corresponds to the Borzai Zone *sensu* Reháková (2000a, b), reflecting a distinct diversification event among calcareous cysts, following the Moluccana interval. According to

Reháková (2000a), the Borzai Zone is restricted to the uppermost Kimmeridgian deposits and does not extend into the Tithonian, an interpretation further supported by Lakova *et al*. (1999), who also assigned this biozone exclusively to the uppermost Kimmeridgian.

Pulla Acme Zone

The next, younger zone recognized in the section corresponds to the Pulla Acme Zone. It is documented within the upper nodular limestones, representing a *Saccocoma–Globochaete* microfacies. Samples from 31 and 31.4 m yield a characteristic cyst assemblage, composed of *Committosphaera pulla* (Fig. 8G), *Colomisphaera carpathica, Col. pieniniensis*, rare *Col. minutissima* (Fig. 8I), *Col. cieszynica*, *Col. ornata* (Fig. 8H) and *Col. lapidosa*. This assemblage defines the Pulla Acme Zone of the Lower Tithonian, as originally proposed by Nowak (1968) on the basis of the FO of *C. pulla*. According to Reháková (2000a), *C. pulla* appeared at the beginning of the Early Tithonian and became abundant prior to the FO of *C. tithonica*. This proliferation event is regarded as an important eco-event.

Malmica Zone

A younger cyst assemblage, characteristic of the Malmica Zone, is documented in the middle part of the upper nodular limestones, at 30 m and 31.7 m of the section. The microfacies are represented by *Saccocoma–Globochaete* wackestones to packstones. The assemblage is dominated by *Parastomiosphaera malmica* (Fig. 8F), particularly abundant within micritic nodules. Associated taxa include *Carpistomiosphaera borzai* (Fig. 8E), *Colomisphaera lapidosa*, *Col. cieszynica*, and rare *Cadosina parvula*. This association defines the Malmica Zone of the upper part of Lower Tithonian (Reháková, 2000a, b). According to Reháková (2000a), the FO of *P. malmica* is used to define this zone, which is further characterized by a high diversity of calcareous dinoflagellate cysts.

Cieszynica Zone

A well-defined cyst association, characteristic of the Cieszynica Zone *sensu* Nowak (1976), is recorded at 32.2 m, within the *Globochaete–Saccocoma* wackestones of the upper nodular limestones. The cyst association is dominated by *Colomisphaera cieszynica* (Fig. 8L), *Col. lapidosa* (Fig. 8J), and *Col. carpathica* (Fig. 8K), with rare occurrences of *Parastomiosphaera malmica* and *Stomiosphaera moluccana*. The Cieszynica Zone is the equivalent of the Semiradiata Zone (introduced by Reháková, 2000a), the zone overlying the Malmica Zone.

Stable isotope data ($\delta^{13}C$ and $\delta^{18}O$)

The stable isotope dataset from the Niedzica-Podmajerz section comprises new 51 bulk carbonate samples spanning the Upper Bajocian to Lower Tithonian interval. The $\delta^{13}C$ values range from +1.7‰ to +3.5‰ VPDB, while $\delta^{18}O$ values vary between –4.4‰ and +0.4‰ VPDB (Fig. 3). In the lower part of the section (lower nodular limestones), $\delta^{13}C$ values show a gradual increase from ~2.0 to ~2.4‰ throughout the first 14 m of the section. Scattered $\delta^{13}C$ values with a negative excursion (down to ~1.8‰) occurs at around 14 m, which corresponds to the tuffite layer, identified by Wierzbowski *et al*. (2012). This excursion is accompanied by a minor decrease in $\delta^{18}O$ values up to –2.3‰.

Above this level in the uppermost part of the lower nodular limestones, both $\delta^{13}C$ and $\delta^{18}O$ values increase, culminating in a pronounced maximum in the interval between ~17 and 18 m, where $\delta^{13}C$ exceeds +3.5‰ and $\delta^{18}O$ rises to +0.4‰. This isotopic peak corresponds to lower nodular limestones with bioclastic, *Globuligerina* and radiolarian microfacies of high carbonate content. From 19 m upward, a gradual decline in $\delta^{13}C$ values is observed within the radiolarites up to 1.7 ‰ in the red radiolarites at 24 m. In radiolarites, $\delta^{18}O$ values remain consistently low (–4‰), suggesting significant diagenetic overprinting of their oxygen isotope composition.

A renewed, modest positive $\delta^{13}C$ excursion (~2.3‰) is recorded in the lower part (~24–27 m) of upper nodular limestones, which is followed by a slight decrease to ~1.8‰. In the uppermost part of the section, spanning the Lower Tithonian, $\delta^{13}C$ values stabilize at similar value, and $\delta^{18}O$ values remain relatively high (average –0.9‰), with no significant long-term trend. The newly obtained $\delta^{13}C$ dataset from the upper nodular limestones and the lowermost part of radiolarites resembles closely the carbon isotope record of the same interval of the Niedzica-Podmajerz section, published by Arabas (2016; see Fig. 3).

DISCUSSION

Integrated stratigraphy

The stratigraphy of the Niedzica-Podmajerz section, from the grey crinoidal limestones up to the boundary with the lower nodular limestones (Bajocian to Callovian–Oxfordian), has been well-established in previous studies (Wierzbowski *et al*., 1999; Krobicki *et al*., 2006b; Arabas, 2016). The present study, built upon this framework by integrating new data from calcareous dinoflagellate cyst assemblages and stable carbon isotope stratigraphy, extends and refines the stratigraphy of the Callovian–Lower Tithonian interval. Each isotopic event and associated microfacies is correlated with specific stratigraphic levels, providing enhanced temporal resolution and insight into palaeoceanographic changes that occurred across the Middle to Late Jurassic transition.

In the analysed material, the relatively low correlation coefficients between $\delta^{18}O$ and $\delta^{13}C$ values, observed in the most carbonate facies suggest minimal diagenetic alteration, whereas its higher values occur in the radiolarites. The $\delta^{18}O$ values of the radiolarites remain consistently low (~ –4.0‰; Fig. 9), indicating their burial-related diagenetic overprint, consistent with the dataset of Arabas (2016). This overprint may also result in slightly reduced $\delta^{13}C$ values of radiolarites (Fig. 9).

The upper part of the lower nodular limestones (*Bositra* microfacies), underlying the prominent $\delta^{13}C$ peak at 17.1 m, were assigned by Arabas (2016) to the Lower Bathonian–Middle Callovian. This notion was based on Lower Bathonian ammonite evidence from subjacent strata (at ca. 14 m;

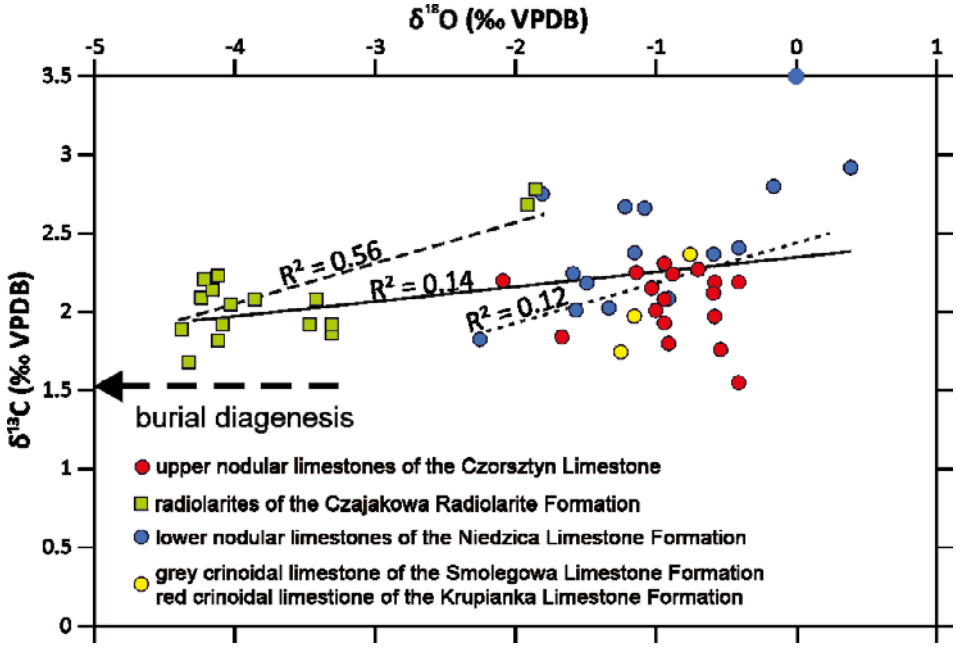

Fig. 9. Correlation diagram between $\delta^{13}C$ and $\delta^{18}O$ values, measured on bulk carbonate samples from the Niedzica-Podmajerz section.

Wierzbowski *et al*., 1999) and on correlation of the local $\delta^{13}C$ curve with other Tethyan records. The overlying beds (17.1–18 m) of the nodular limestones, characterized by elevated $\delta^{13}C$ values, were broadly defined as Upper Callovian–Middle Oxfordian (Arabas, 2016).

It is noteworthy that the topmost part (17.2–18 m) of the lower nodular limestones, positioned above the major $\delta^{13}C$ peak, contains a *Globuligerina* microfacies (Krobicki *et al*., 2006a), which has been linked to the uppermost Callovian–Lower Oxfordian interval in the Niedzica Succession. Bioclastic wackestones with *Chondrites* isp. and *Colomisphaera fibrata* at 17.2 m, have been presently assigned to the Fibrata Zone (*sensu* Lakova, 1993) of the Oxfordian. Approximately 20 cm below the top lower nodular limestones in the Czajakowa Klippe section, radiolarian assemblages record a transition from UAZ 8 (Middle Callovian–Early Oxfordian) to UAZ 9 (Middle–Late Oxfordian; Bąk *et al*., 2018). Thus, the boundary between the Lower and Middle Oxfordian should be recorded in the uppermost part of the lower nodular limestones of the Niedzica-Podmajerz section. These data seem to be inconsistent with previous chemostratigraphical dating of the rocks.

Detailed isotope data indicate, however, that the Upper Callovian carbon isotope excursion persisted actually until the Mariae Chron of the earliest Oxfordian and was followed by another Middle Oxfordian excursion (Wierzbowski, 2015). This reconciles the apparent discrepancy between the isotope chemostratigraphy with the calcareous dinoflagellate cyst zonation. The observed positive $\delta^{13}C$ excursion corresponds, thus, to the Late Callovian carbon isotope event, widely documented in Tethyan and Peri-Tethyan successions, which is sometimes extended to the Early Oxfordian (Weissert and Mohr, 1996; Cecca *et al*., 2001; Jach *et al*., 2014; Pellenard *et al*., 2014; Wierzbowski, 2015). Moreover, the lithological character of the discussed interval (see below, the section Sedimentary environment, *Lower nodular limestones*), the rapid rise of the carbon isotope curve between 16.6 and 17.1 m and its abrupt decrease between 17.2 and 18.0 m collectively suggest an occurrence of the condensed intervals with possible hiatus(es).

Above 18 m, $\delta^{13}C$ values show a steady decline from ~3.5‰ to ~1.7‰ by 24 m (Fig. 3). This negative trend spans the uppermost ~0.3 m of the lower red nodular limestones and continues into the overlying radiolarites. The absence of the characteristic Middle Oxfordian positive $\delta^{13}C$ excursion (cf. Wierzbowski, 2015; Feldman-Olszewska *et al*., in press) likely reflects condensation and stratigraphic discontinuities at the nodular limestone–radiolarite contact. Supporting this interpretation are signs of bioclast phosphatization, documented in the lowermost radiolarites (sample Po 18.7). The same sample contains *Committosphaera czestochowiensis*, the known range of which extends from the Lower to Middle Oxfordian (Olszewska, 2010).

The overlying green and upper red radiolarites in the studied section have been assigned to UAZ 9–10 (Widz, 1991; Birkenmajer and Widz, 1995), corresponding to the Middle Oxfordian–Lower Kimmeridgian. This upper interval displays a pronounced negative $\delta^{13}C$ trend, characteristic of many Tethyan successions for the Upper Oxfordian and preceding the onset of the Kimmeridgian positive excursion (Bartolini *et al*., 1996, 1999; Cecca *et al*., 2001; Jenkyns *et al*., 2002).

A stratigraphically important assemblage occurs between 24.7–24.8 m in the lowermost part of the upper nodular limestones, which consists of thin-bedded red limestones with *Saccocoma*-filamentous packstones. This interval is characterized by a calcareous cyst assemblage, dominated by *Cadosina parvula*, accompanied by *Colomisphaera carpathica* and *Col. minutissima*, defining the Parvula Acme Zone (*sensu* Reháková, 2000a), which is considered to correspond to the Lower Kimmeridgian. It serves as a useful biostratigraphic marker for correlating pelagic deposits

across the Alpine-Carpathian region (e.g., Reháková, 2000a; Ivanova and Kietzmann, 2017).

Within the lower part of the upper red nodular limestones (24.8–27.5 m), another modest positive $\delta^{13}C$ shift (to ~2.3‰) is recorded. These beds contain *Saccocoma*-filamentous packstones, and represent typical pelagic facies, deposited on the outer slope of the Czorsztyn Ridge. The presence of *Stomiosphaera moluccana* along with *Colomisphaera pieniniensis* and *Col. carpathica* allows assignment to the Moluccana Zone. This positive shift corresponds to the secondary Kimmeridgian carbon isotope excursions, observed in the Western Tethys (cf. Bartolini *et al*., 1996, 1999; Cecca *et al*., 2001; Grabowski *et al*., 2019). High $\delta^{13}C$ values of bulk-carbonates are also reported from the lowermost and the uppermost Lower Kimmeridgian of the southern part of the Polish epicontinental basin (Feldman-Olszewska *et al*., in press).

A minor negative $\delta^{13}C$ shift (~1.8‰) is recorded at ~27.5 m, in the upper part of the upper nodular limestones. A similar shift has been reported in other Carpathian sections (Jach *et al*., 2014; Grabowski *et al*., 2019). This level marks the FO of *Carpistomiosphaera borzai*, associated with *Stomiosphaera moluccana*, indicating the base of the Borzai Zone. This interval corresponds to Rosso Ammonitico-type facies with low sedimentation rates. The isotopic signal at this level may reflect a transient decrease in surface productivity or enhanced organic matter oxidation, occurring during a phase of palaeoceanographic instability at the Kimmeridgian–Tithonian transition.

Above 28.5 m, $\delta^{13}C$ values stabilize around 1.8‰ and remain consistent through the upper part of the upper nodular limestones. This stability coincides with a broader, long-term downward trend in $\delta^{13}C$, documented for marine carbonates of Kimmeridgian–Tithonian age in the Tethyan realm (Weissert and Channell, 1989; Cecca *et al*., 2001; Padden *et al*., 2002; Jach *et al*., 2014; Michalík *et al*., 2016; Price *et al*., 2016; Grabowski *et al*., 2017, 2019). Such a pattern is generally attributed to a global reduction in the burial of marine organic carbon and/or an increase in carbonate production (Weissert and Channell, 1989; Weissert *et al*., 1998; Price *et al*., 2016). Lithologically, this part of the section is dominated by red nodular limestones, containing *Saccocoma*-filamentous packstones and *Globochaete-Saccocoma* wackestones to packstones, representing stable pelagic sedimentation under low accumulation rates. Calcareous dinoflagellate cyst assemblages correspond to the Pulla, Malmica and Cieszynica zones (Early Tithonian), although the stratigraphic overlap of the Pulla Zone within the Malmica Zone may reflect subtle reworking or tectonic activity, possibly related to the occurrence of neptunian dykes.

The $\delta^{13}C$ curve of the Niedzica-Podmajerz section shows a high degree of consistency with the isotope record of the Długa Valley section in the Tatra Mountains, enabling correlation of major isotopic events across the Bathonian–Lower Tithonian interval (Fig. 10; Jach *et al*., 2014; Jach, 2021). The most prominent feature of the Tatra dataset is a positive carbon isotope excursion, spanning the Upper Callovian to the Middle Oxfordian. Furthermore, the overall decreasing $\delta^{13}C$ trend from the Middle Oxfordian to the Lower Tithonian constitutes a significant element, reinforcing this correlation. A similar isotopic trend has been reported also from pelagic carbonate successions, spanning the Callovian–Tithonian interval in the Trapani area of western Sicily (Cecca *et al*., 2001). A minor negative carbon isotope shift is observed near the Kimmeridgian–Tithonian boundary in both the Tatra Mountains and the Trapani area, which follows a broader positive anomaly that characterises much of the Kimmeridgian.

Sedimentary environment

During the Middle–Late Jurassic, the Czorsztyn Ridge formed a prominent intrabasinal high within the Pieniny Basin (Fig. 1; Birkenmajer, 1977; Krobicki *et al*., 2006b). Sedimentation on the Jurassic ridges and their slopes encompassed a spectrum of pelagic carbonate facies, from high-energy crinoidal limestones and fully pelagic Rosso Ammonitico-type nodular facies on elevated settings to fine-grained marly limestones and radiolarites in deeper, more quiescent environments (Bernoulli and Jenkyns, 1974; Birkenmajer, 1977; Santantonio, 1993; Martire, 1996; Jach and Reháková, 2019). These facies patterns were shaped by relative sea-level changes, tectonically induced subsidence, and variations in carbonate production, with periodic influxes of terrigenous material and redeposited bioclasts from nearby submarine ridges to basins (Bernoulli and Jenkyns, 1974; Clari and Martire, 1996). Basin-scale palaeoceanographic processes, including fluctuations in nutrient supply and carbonate saturation, further modulated the distribution of facies belts (FZ 1–4) and microfacies types (MF 1–6) across the ridge-to-basin transect (Fig. 11).

Crinoidal limestones

The grey crinoidal limestones of the Smolegowa Limestone Formation in the Niedzica succession accumulated in a well-oxygenated, moderately agitated marine setting, which prevailed on the slope of an already uplifted submarine ridge. Their grain-supported textures (packstones-grainstones) and predominance of disarticulated crinoid ossicles with only rare pluricolumnals indicate redeposition below the fair-weather wave base (Fig. 11; FZ 4 – slope; Głuchowski, 1987; Łuczyński, 2002). This interpretation is supported by the presence of numerous benthic foraminifera, including taxa indicative of shallow-marine origins, together with pelagic elements, such as ammonites, belemnites, and calcareous dinoflagellate cysts, indicating deposition in the transitional zone between the shallow ridge and the deeper pelagic conditions.

Comparable shallow-water crinoidal facies have been described from the Hatné-Hrádok locality in the Czorsztyn Unit, where cross-bedding, good sorting, winnowing of micrite, and abrasion of crinoidal ossicles demonstrate sedimentation above the wave base within crinoidal shoal deposits (Aubrecht and Sýkora, 1998). These observations highlight that Smolegowa-type limestones in the Niedzica-Podmajerz section represent slightly deeper and more distal equivalents of such high-energy shoal deposits. Crinoid ossicles display partial abrasion and fragmentation, suggesting short- to moderate-distance transport from nearby crinoid meadows and final deposition in a more distal

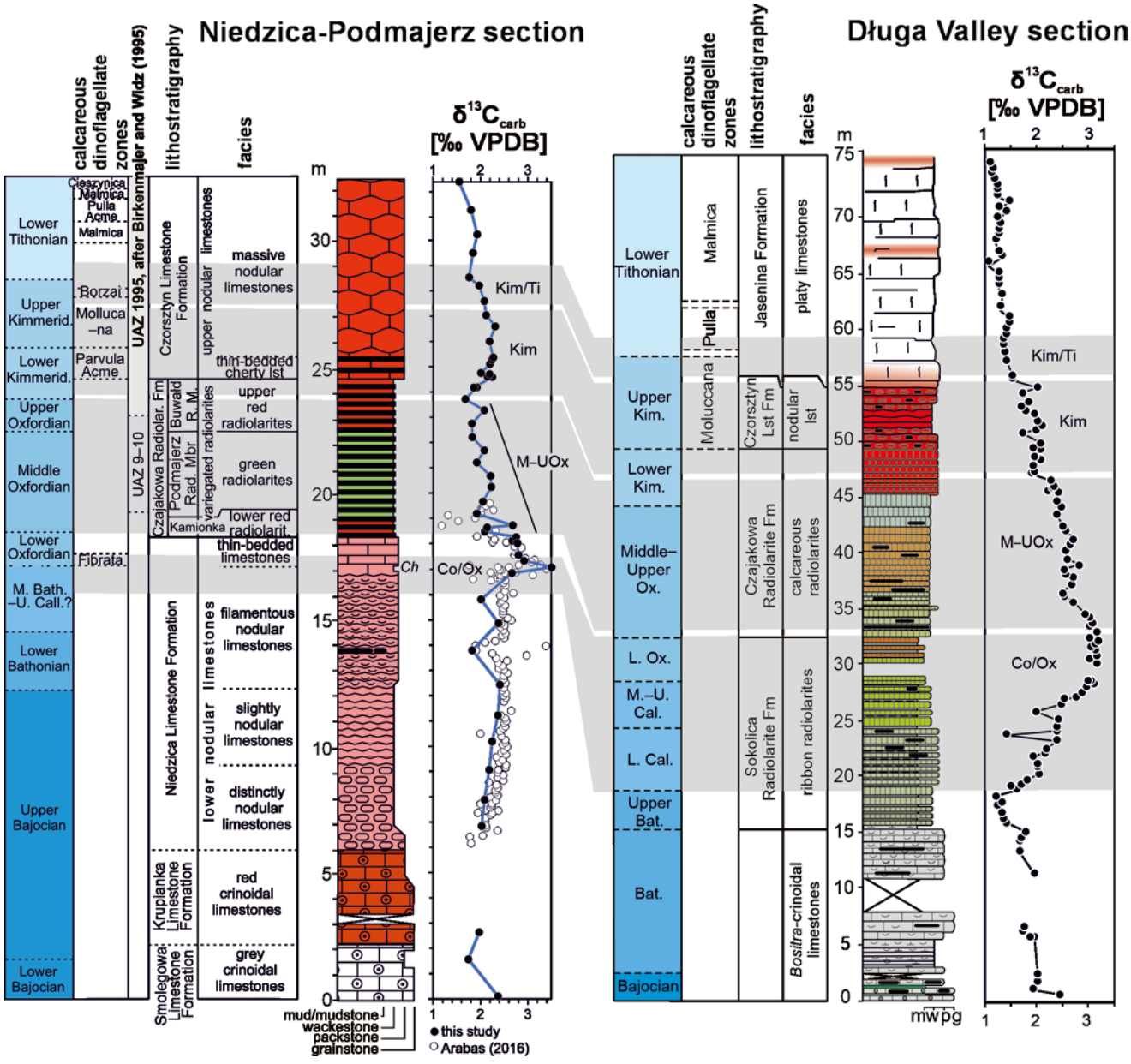

Fig. 10. Comparison of $\delta^{13}C$ and $\delta^{18}O$ records from Niedzica-Podmajerz section and Długa Valley section (Tatra Mts.; Jach *et al*., 2021), highlighting consistent trends across the Middle–Upper Jurassic.

setting, located basinward of the meadows, corresponding to zone Z2b (*sensu* Głuchowski, 1987). This interpretation aligns with Blyth Cain's (1968) and Jenkyns' (1971a) observations that even moderate displacement can abrade and disarticulate delicate crinoid skeletons.

The occurrence of sand-sized siliciclastic and carbonate lithoclasts reflects episodic input from fault-controlled submarine highs that were intermittently eroded and shed material downslope. Also, the occurrence of the trace fossil *Curvolithus* isp., documented by Krobicki and Uchman (2003), provides support for slope deposition, as this ichnotaxon typically forms below the fair-weather wave base and is associated with the distal toes of migrating crinoid shoals.

The overlying red crinoidal limestones of the Krupianka Limestone Formation record progressive deepening and reduced energy toward distal slope conditions (Fig. 11; FZ 4; Wierzbowski *et al*., 1999). Glauconite and bored bioclasts

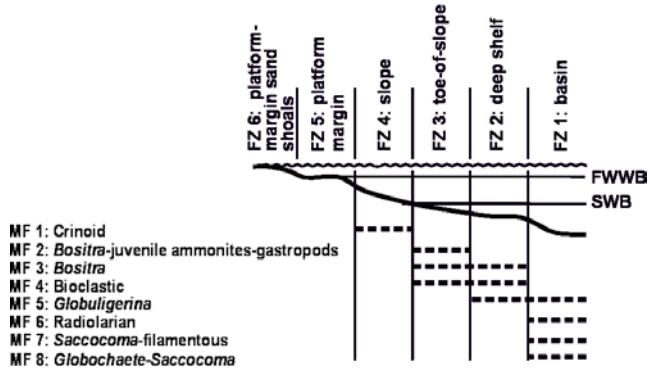

Fig. 11. Distribution of microfacies types (MF) within facies zones (FZ) across different parts of the carbonate shelf, after Wilson (1975) and Flügel (2004), modified according to microfacies data from the Niedzica-Podmajerz section. Legend: FWWB – fair-weather wave base, SWB – storm wave base.

suggest a slow sedimentation rate and prolonged residence of skeletal debris on the seafloor before burial. These features, together with fine grain size, point to deposition beneath the storm wave base in a low-energy open-marine setting. Similar depositional trends have been described from the Tatricum Basin (Łuczyński, 2002, 2021) and Fatricum domain (Iwańczuk *et al*., 2013; Jach and Reháková, 2019), where crinoidal debris, derived from platform-margin shoals, was transported basinward by density currents.

Lower nodular limestones

Lower nodular limestones (Niedzica Limestone Formation) in the Niedzica-Podmajerz section record a progressive deepening trend along the slope of the Czorsztyn Ridge (Wierzbowski *et al*., 1999). This transition from toe-of-slope to basinal conditions (FZ 3–1; Fig. 11) reflects the interplay of terrigenous and bioclastic input, productivity fluctuations, and episodic high-energy events, consistent with patterns, documented in other Tethyan slope successions (Santantonio, 1993; Clari and Martire, 1996).

In the lower nodular interval (6–9.2 m; MF 2), loosely packed nodules in a marly matrix with filamentous bivalves, juvenile ammonites, gastropods, and rare crinoids indicate pelagic deposition below the storm wave base (FZ 3). Intensely bored and phosphatized bioclasts at the base of the section (samples Po 6.1 and Po 8.3) point to a slow sedimentation rate and early diagenetic phosphate precipitation in organic-rich microenvironments, a feature typical of condensed pelagic carbonates (Rao *et al*., 2008; Benites *et al*., 2021).

The overlying *Bositra*-rich limestones (9.2–17.0 m) record enhanced *in situ* productivity in the vicinity of ridge-type topography, where *Bositra*, a small, opportunistic suspension feeder (Wignall, 1993; Caswell and Coe, 2013; Molina *et al*., 2018), could proliferate in aphotic, nutrient-limited settings, sustained by episodic nutrient injections from internal waves (Tomašových *et al*., 2020). The overwhelming dominance of *Bositra* shells, often exceptionally large and well-preserved, suggests rapid accumulation of autochthonous material with minimal post-mortem transport. In contrast, intervals showing grading, shell imbrication, or disordered fabrics point to episodic reworking by bottom currents or storm-induced flows. Comparable shell concentrations were formed during carbonate production crises and condensation events in other Tethyan basins (Santantonio, 1993; Clari and Martire, 1996; Jach, 2007; Navarro *et al*., 2009, 2012; Vörös, 2012; Jach and Reháková, 2019), reflecting the combined effects of ecological opportunism, hydrodynamic sorting, and sediment starvation.

The upper nodular interval (17–18.2 m) marks a shift to fully basinal conditions (FZ 1), with microfacies evolving from *Bositra* packstone to wackestones (MF 3) to bioclastic (MF 4), *Globuligerina* (MF 5), and radiolarian-rich wackestones (MF 6). This change indicates the decline of the benthic carbonate factory and the onset of plankton-dominated sedimentation, coinciding with a prominent positive $\delta^{13}C$ excursion linked to Upper Callovian–Lower Oxfordian carbon-cycle perturbations (Weissert and Mohr, 1996; Cecca *et al*., 2001; Pellenard *et al*., 2014; Wierzbowski, 2015). The steep gradient of the $\delta^{13}C$ curve in the studied section may also be linked to a low sedimentation rate and a possible hiatus, similar to that reported from the Velykyi Kamianets section, where the Middle Callovian–Lower Oxfordian interval is missing (Lewandowski *et al*., 2005; Reháková *et al*., 2011).

The red micritic limestone at 17.1 m, densely bioturbated with *Chondrites* isp., likely records extremely slow sedimentation or even a brief hiatus. Such deposits form under prolonged seafloor exposure and reduced sediment input, enabling sustained colonisation by deposit-feeding organisms (Bromley, 1975; Bromley and Ekdale, 1984). Phosphatised bioclasts, microbial oncoids, and reworked lithoclasts indicate repeated winnowing, and extended residence at or near the sediment-water interface (Jach and Starzec, 2003; Christ *et al*., 2012; Benites *et al*., 2021). These features suggest deposition on a pelagic ridge during sediment starvation, with intermittent nutrient fluxes and bottom-current activity, alternating with low-energy, oxygen-poor bottom waters. The occurrence of *Chondrites* isp. within the highest $\delta^{13}C$ interval may reflect the colonisation of firmgrounds or omission surfaces, followed by truncation of shallow-tier structures (Bromley, 1975; Santantonio, 1993; Christ *et al*., 2012).

The overall thinness of the Middle Bathonian–Lower Oxfordian interval (~3 m), compared to the radiolarite-rich basinal successions (up to 20 m in the Branisko Succession; Krobicki *et al*., 2006c), reflects persistent hydrodynamic winnowing on ridge slopes, which hindered radiolarian accumulation. Similar patterns are observed in other Tethyan basins, where radiolarites preferentially accumulated in deeper, sheltered depocentres (Baumgartner, 1987).

Radiolarites

The shift from pelagic carbonate to siliceous, radiolarian-rich sedimentation marks a distinct change in depositional style. This lithological trend is interpreted as a long-term reduction in regional-surface carbonate productivity, which is consistent with the palaeoceanographic changes, documented in other Tethyan basins (Bartolini *et al*., 1996, 1999; Baumgartner, 1987, 2013).

The variegated radiolarites of the Czajakowa Radiolarite Formation record deep-water pelagic sedimentation, dominated by radiolarian fallout. Rare crinoid debris and faint grading indicate episodic allochthonous input from proximal settings via dilute gravity flows. The succession, corresponding to radiolarian wackestones and packstones (MF 6), formed in a basinal environment (FZ 1; Fig. 11). The fine, locally laminated texture and fluctuating, but generally low terrigenous input reflect the settling of siliceous radiolarian tests, important components of marine snow, although Kwiatkowski (1981) interpreted the radiolarites of the Niedzica Succession as the products of bottom-current activity, influenced by fluctuating clay input and radiolarian productivity, with early diagenetic separation of silica and carbonate phases.

Radiolarite accumulation in the Pieniny Basin was favoured by low sedimentation rates, focused biogenic silica flux, and sediment trapping beneath persistently productive surface waters. In the Tethyan realm, radiolarite facies commonly developed under elevated productivity, linked to seasonal or monsoon-driven upwelling (Baumgartner, 2013;

De Wever *et al*., 2014). The predominance of radiolarians, scarcity of detrital input, and locally the preservation of fine lamination in the Niedzica-Podmajerz section are consistent with deposition in a distal passive-margin basin beneath zones of sustained biogenic silica production.

A pronounced vertical trend is observed – carbonate-rich lower red radiolarites pass upward into strongly siliceous green radiolarites, followed by a partial return to carbonate-bearing upper red radiolarites. This pattern reflects long-term shifts in the aragonite lysocline, aragonite compensation depth (ACD), calcite lysocline, and calcite compensation depth (CCD), similar to successions in the Southern Alps, where carbonate preservation was controlled by CCD/ACD fluctuations (Bosellini and Winterer, 1975; Winterer and Bosellini, 1981). In the Niedzica-Podmajerz section, the preservation of calcitic aptychi and the absence of aragonitic ammonites provide taphonomic evidence for past ACD and CCD positions. Moreover, the aptychi stratigraphic framework, established by Gąsiorowski (1962) for the PKB, remains an invaluable source of biostratigraphic information, offering essential context for interpreting these palaeoceanographic signals. The lower and upper red radiolarites, retaining calcareous microfossils (aptychi, filaments, calcareous dinoflagellate cysts, *Globochaete*), likely accumulated between the ACD and calcite lysocline, whereas the green radiolarites, with minimal $CaCO_3$ (mean value 33%, dropping locally to 5%; Fig. 3) and an absence of calcareous fossils, reflect shoaling of the CCD to the seafloor. Since a $CaCO_3$ content of 20% is commonly taken as an arbitrary threshold for deposits, formed below the CCD (*sensu* Bostock *et al*., 2011), part of the Middle Oxfordian radiolarites (Fig. 3) could potentially have been deposited beneath this depth. Interestingly, the high $CaCO_3$ contents, recorded at the top of the green radiolarites, may at least partly reflect downslope transport and input of carbonate material. The subsequent return to carbonate preservation in the upper interval suggests a relative deepening of the CCD.

Although CCD and ACD indicators provide valuable palaeoceanographic insights, they represent dynamic horizons, the depth of which fluctuates in response to changes in ocean chemistry (pCO_2, carbonate saturation state), productivity, deep-water circulation, and carbonate flux (Rea and Lyle, 2005; Bostock *et al*., 2011). Local tectonic movements, such as subsidence or uplift, may further modify their position, relative to the seafloor. Consequently, depth estimates, based on these markers, must be interpreted cautiously within a broader palaeoceanographic and tectonic framework. It is well established that the CCD depth can vary markedly within a single basin and may shift independently in neighbouring isolated or semi-isolated basins (Lee *et al*., 2000; Bostock *et al*., 2011; De Wever *et al*., 2014). Therefore, in the present study, inferred CCD shoaling and deepening are regarded as qualitative trends, rather than precise bathymetric indicators, reflecting general changes in carbonate preservation potential, rather than absolute depth fluctuations.

Upper nodular limestones

Within the Alpine-Mediterranean Tethys, red nodular limestones represent one of the most distinctive Jurassic facies, with comparable lithotypes also documented from various other geological intervals (Bernoulli and Jenkyns, 1974; Tucker, 1974). They are typically associated with sedimentation under exceptionally low accumulation rates (Jenkyns, 1974; Tucker, 1974; Martire, 1996). The preservation of an uncompacted nodule fabric points to early diagenetic cementation, probably initiated at very shallow burial levels, close to the sediment-water interface. This process probably was driven by a combination of hydrodynamic activity, hydrodynamic winnowing, pore-water circulation, bioturbation, dissolution of aragonite, and the onset of cement precipitation (Jenkyns, 1974; Clari and Martire, 1996; Bertok and Martire, 2009; Coimbra *et al*., 2009; Reolid *et al*., 2015).

Throughout the Tethys, including the studied section, the latest Kimmeridgian to Early Tithonian marked a return to carbonate-dominated sedimentation, expressed in red thin-bedded limestones of the Rosso ad Aptici-type facies and in the nodular limestones, characteristic of the Rosso Ammonitico (Jenkyns, 1971b; Martire, 1996). These deposits formed well below the storm wave base (FZ 1), most commonly on pelagic ridges, but also on adjacent slopes and in basinal settings, where similarly low-energy conditions favoured the development of condensed pelagic successions (Birkenmajer, 1977; Cecca *et al*., 1992; Wierzbowski *et al*., 1999; Jach and Reháková, 2019).

The observed shift from radiolarian-dominated microfacies in deeper basins, or *Globuligerina* microfacies on ridges and slopes, to *Saccocoma*-rich facies reflects a broader Kimmeridgian facies transition, documented across the PKB and the Western Tethys (Wierzbowski *et al*., 1999; Reháková *et al*., 2011; Benzaggagh, 2015; Grabowski *et al*., 2019). This transition was likely linked to climatic changes and associated alterations in the trophic state of the basin, reflecting a fundamental reorganisation of nutrient cycling and primary productivity, with a decline in siliceous plankton production and a relative increase in carbonate-secreting biota. The abundance of *Saccocoma* indicates mesotrophic to eutrophic conditions below the storm wave base, typical of late Kimmeridgian to early Tithonian highstand intervals (Matyszkiewicz, 1996; Flügel, 2004; Piuz, 2008). A similar relationship was identified by Lodowski *et al*. (2024), who argued that the disappearance of *Saccocoma* coincided with climate aridization, which enhanced water-column stratification and reduced the supply of micronutrients to the surface waters.

Palaeoenvironmental turning points

The Niedzica-Podmajerz section preserves a sequence of significant Middle–Late Jurassic palaeoenvironmental shifts, reflecting long-term changes in bathymetry, carbonate production, and oceanographic regime. The first marks the replacement of the crinoidal limestones by the lower nodular limestones, indicating the decline of the benthic crinoid factory, reduced sedimentation rates, progressive deepening, and a faunal turnover from shallow-water crinoids to *Bositra*-dominated deeper-water assemblages, periodically affected by pelagic input. The second, in the Bathonian–Oxfordian, records the transition from *Bositra*-rich wackestones (MF3) to plankton-dominated

microfacies (MF5–MF6), signalling fully pelagic, deep-basin sedimentation (FZ1) and coinciding with the prominent Upper Callovian–Lower Oxfordian positive $\delta^{13}C$ excursion. The next shift corresponds to the onset of variegated radiolarites, reflecting a phase of enhanced siliceous productivity and intensified carbonate dissolution. Green radiolarites, lacking calcareous fossils, may indicate deposition under conditions of reduced carbonate preservation, possibly close to the CCD. The final turning point marks the return to red nodular limestones with *Saccocoma* and *Globochaete*, signalling renewed pelagic-carbonate accumulation and the establishment of a condensed Rosso Ammonitico-type regime, marking the end of the Late Jurassic carbonate-production crisis.

CONCLUSIONS

The Niedzica-Podmajerz section preserves a nearly continuous record of pelagic sedimentation from the Upper Bajocian to the Early Tithonian, representing a high-resolution archive of palaeoenvironmental and stratigraphic change along the northern Tethyan margin.

The integration of sedimentological, microfacies, and geochemical data indicates a long-term deepening trend from the Early Bajocian to the Oxfordian, spanning a transition from crinoidal slope deposits (the grey and red crinoidal limestones of the Smolegowa and Krupianka formations), through the condensed lower nodular limestones of the Niedzica Limestone Formation, to the pelagic radiolarites of the Czajakowa Radiolarite Formation. This trend culminated in maximum flooding and was followed by the high-stand deposition of the nodular limestones of the Czorsztyn Limestone during the Kimmeridgian–Lower Tithonian.

Stable carbon isotope data ($\delta^{13}C$) document global palaeoceanographic events, including a major positive excursion in the Upper Callovian–lowermost Oxfordian (up to +3.5‰), correlated with enhanced productivity and transgressive conditions, followed by a long-term decline of the $\delta^{13}C$ through the Oxfordian–Kimmeridgian, punctuated by second-order fluctuations at the Parvula and Moluccana zones.

Calcareous dinoflagellate cysts provide a robust biostratigraphic framework, with recognition of seven key zones (Fibrata, Parvula, Moluccana, Borzai, Pulla, Malmica and Cieszynica), allowing refinement of the age of the section and its correlation with other Alpine–Carpathian successions. Their stratigraphic ranges are consistent with isotopic trends and facies shifts.

The combined use of classical biostratigraphy (ammonites, aptychi), modern micropalaeontological proxies (calcareous dinoflagellate cysts), and carbon isotope stratigraphy establishes the Niedzica-Podmajerz section as a regional reference section for the Jurassic of the PKB and the broader Western Tethys.

Acknowledgements

The work was supported by a grant from the Faculty of Geography and Geology under the Priority Research Area (Anthropocene) of the Strategic Programme Excellence Initiative at the Jagiellonian University. DR was supported by Project of the Slovak Grant Agency No. APVV-20- 0079. We are grateful to Andrzej Wierzbowski for his constructive comments. We sincerely thank Michał Krobicki for his exceptionally helpful review and the anonymous reviewer for valuable comments and suggestions. Grateful thanks to Józef Milaniak for logistical support and assistance with fieldwork.

REFERENCES

Arabas, A., 2016. Middle–Upper Jurassic stable isotope records and seawater temperature variations: New palaeoclimate data from marine carbonate and belemnite rostra (Pieniny Klippen Belt, Carpathians). *Palaeogeography, Palaeoclimatology, Palaeoecology*, 446: 284–294.

Aubrecht, R. & Sýkora. M., 1998. Middle Jurassic crinoidal shoal complex at Hatné - Hrádok locality (Czorsztyn Unit, Pieniny Klippen Belt, Western Slovakia). *Mineralia Slovaca*, 30: 157–166.

Bąk, M., Chodacka, S., Bąk, K. & Okoński, S., 2018. New data on the age and stratigraphic relationships of the Czajakowa Radiolarite Formation in the Pieniny Klippen Belt (Carpathians) based on the radiolarian biostratigraphy in the stratotype section. *Acta Geologica Polonica*, 68: 1–20.

Bartolini, A., Baumgartner, P. & Guex, J., 1999. Middle and Late Jurassic radiolarian palaeoecology versus carbon-isotope stratigraphy. *Palaeogeography, Palaeoclimatology, Palaeoecology*, 145: 43–60.

Bartolini, A., Baumgartner, P. & Hunziker, J., 1996. Middle and Late Jurassic carbon stable isotope stratigraphy and radiolarite sedimentation of the Umbria–Marche basin (central Italy). *Eclogae Geologicae Helvetiae,* 89: 811–844.

Bartolini, A. & Cecca, F., 1999. 20 My hiatus in the Jurassic of Umbria-Marche Apennines (Italy): carbonate crisis due to eutrophication. *Comptes Rendus de l'Académie des Sciences. Série 2, Sciences de la Terre et des Planètes*, 329: 587–595.

Baumgartner, P. O., 1987. Age and genesis of Tethyan Jurassic radiolarites. *Eclogae Geologicae Helvetiae*, 80: 831–879.

Baumgartner, P. O., 2013. Mesozoic radiolarites – Accumulation as a function of sea surface fertility on Tethyan margins and in ocean basins. *Sedimentology*, 60: 292–318.

Benites, M., Hein, J. R., Mizell, K. & Jovane, L., 2021. Miocene phosphatization of rocks from the summit of Rio Grande Rise, Southwest Atlantic Ocean. *Paleoceanography and Paleoclimatology*, 36: e2020PA004197.

Benzaggagh, M., Homberg, C., Schnyder, J. & Ben Abdesselam-Mahdaoui, S., 2015. Description et biozonation des sections de crinoïdes saccocomidés du Jurassique supérieur (Oxfordien–Tithonien) du domaine téthysien occidental. *Annales de Paléontologie*, 101: 95–117

Bernoulli, D. & Jenkyns, H. C., 1974. Alpine, Mediterranean and Central Atlantic Mesozoic facies in relation to the early evolution of the Tethys. In: Dott, R. H. & Sharer, R. H. (eds), *Modern and Ancient Geosynclinal Sedimentation. Society of Economic Paleontologists and Mineralogists, Special Publication*, 19: 129–160.

Bertok, C. & Martire, L., 2009. Sedimentation, fracturing and sliding on a pelagic plateau margin: the Middle Jurassic to Lower

Cretaceous succession of Rocca Busambra (Western Sicily, Italy). *Sedimentology*, 56: 1016–1040.

Birkenmajer, K., 1977. Jurassic and Cretaceous lithostratigraphic units of the Pieniny Klippen Belt, Carpathians, Poland. *Studia Geologica Polonica*, 45: 1–158.

Birkenmajer, K., 1986. Stages of structural evolution of the Pieniny Klippen Belt, Carpathians. *Studia Geologica Polonica*, 88: 7–32.

Birkenmajer, K. & Myczyński, R., 1984. Fauna and age of Jurassic nodular limestones near Niedzica and Jaworki (Pieniny Klippen Belt, Carpathians, Poland*). Studia Geologica Polonica*, 83: 7–24. [In Polish, with English summary.]

Birkenmajer, K. & Widz, D., 1995. Biostratigraphy of Upper Jurassic radiolarites in the Pieniny Klippen Belt, Carpathians. In: Baumgartner, P. O., O'Dogherty, L., Goričan, Š., Urquhart, E., Pillevuit, A. & De Wever, P. (eds)*, Middle Jurassic to Lower Cretaceous radiolaria of Tethys: occurrences, systematics, biochronology. Mémoires de Géologie*, *Lausanne,* 23: 889–896.

Birkenmajer, K. & Znosko, J., 1955. Contribution to the stratigraphy of the Dogger and Malm in the Pieniny Klippen Belt (Central Carpathians). *Rocznik Polskiego Towarzystwa Geologicznego*, 23: 3–36. [In Polish, with English summary.]

Blyth Cain, J. D., 1968. Aspects of the depositional environment and palaeoecology of the crinoidal limestones. *Scottish Journal of Geology*, 4: 191–208.

Bosellini, A. & Winterer, E. L., 1975. Pelagic limestone and radiolarite of the Tethyan Mesozoic: A genetic model. *Geology*, 3: 279–282.

Bostock, H. C., Hayward, B. W., Neil, H. L., Currie, K. I. & Dunbar, G. B., 2011. Deep-water carbonate concentrations in the southwest Pacific. *Deep-Sea Research I*, 58: 72–85.

Bromley, R. G., 1975. Trace fossils at omission surfaces. In: Frey, R. W. (ed.), *The Study of Trace Fossils.* Springer, New York, pp. 399–428.

Bromley, R. G. & Ekdale, A. A., 1984. *Chondrites*: a trace fossil indicator of anoxia in sediments. *Science*, 224: 872–874.

Caswell, B. A. & Coe, A. L., 2013. Primary productivity controls on opportunistic bivalves during Early Jurassic oceanic deoxygenation. *Geology*, 41: 1163–1166.

Cecca, F., Bérengére, S., Bartolini, A., Remane, J. & Cordey, F., 2001. The Middle Jurassic–Lower Cretaceous Rosso Ammonitico succession of Monte Inici (Trapanese domain, western Sicily): sedimentology, biostratigraphy and isotope stratigraphy. *Bulletin de la Société Géologique de France*, 172: 647–660.

Cecca, F., Fourcade, E. & Azéma, J., 1992. The disappearance of the "Ammonitico Rosso". *Palaeogeography, Palaeoclimatology, Palaeoecology*, 99: 55–70.

Cecca, F., Martin Garin, B., Marchand, D., Lathuiliere, B. & Bartolini, A., 2005. Paleoclimatic control of biogeographic and sedimentary events in Tethyan and peri-Tethyan areas during the Oxfordian (Late Jurassic). *Palaeogeography, Palaeoclimatology, Palaeoecology*, 222: 10–32.

Christ, N., Immenhauser, A., Amour, F., Mutti, M., Tomas, S., Agar, S. M., Alway, R. & Kabiri, L., 2012. Characterization and interpretation of discontinuity surfaces in a Jurassic ramp setting (High Atlas, Morocco). *Sedimentology*, 59: 249–290.

Clari, P. A. & Martire, L., 1996. Interplay of cementation, mechanical compaction, and chemical compaction in nodular limestones of Rosso Ammonitico Veronese (Middle–Upper Jurassic, northeastern Italy). *Journal of Sedimentary Petrology*, 66: 447–458.

Coimbra, R., Immenhauser, A. & Olóriz, F., 2009. Matrix micrite $\delta^{13}C$ and $\delta^{18}O$ reveals synsedimentary marine lithification in Upper Jurassic Ammonitico Rosso limestones (Betic Cordillera, SE Spain). *Sedimentary Geology*, 219: 332–348.

De Wever, P., O'Dogherty, L. & Goričan, Š., 2014. Monsoon as a cause of radiolarite in the Tethyan realm. *Comptes Rendus Geoscience*, 346: 287–297.

Dunham, R. J., 1962. Classification of carbonate rocks according to depositional texture. In: Ham, W. E. (ed.), *Classification of Carbonate Rocks. A Symposium. American Association of Petroleum Geologists, Memoire*, 1: 108–121.

Erba, E. & Tremolada, F., 2004. Nannofossil carbonate fluxes during the Early Cretaceous: Phytoplankton response to nutrification episodes, atmospheric CO_2, and anoxia. *Paleoceanography*, 19: 1–18.

Feldman-Olszewska, A., Pieńkowski, G., Wierzbowski, H., Wierzbowski, A. & Grabowski, J. (in press). Jura – Niż Polski i pas wyżyn. In: Peryt, T. (ed.), *Budowa geologiczna Polski, Tom 1: Stratygrafia*. Państwowy Instytut Geologiczny – Państwowy Instytut Badawczy, Warszawa. [In Polish.]

Flügel, E., 2004. *Microfacies of Carbonate Rocks, Analysis, Interpretation and Application*. Springer-Verlag, Berlin, 976 pp.

Gąsiorowski, S. M., 1962. Aptychi from the Dogger, Malm and Neocomian in the Western Carpathians and their stratigraphical value. *Studia Geologica Polonica*, 10: 1–151.

Głuchowski, E., 1987. Jurassic and Early Cretaceous articulate Crinoidea from the Pieniny Klippen Belt, and the Tatra Mts., Poland. *Studia Geologica Polonica* 94: 1–102.

Grabowski, J., Bakhmutov, V., Kdýr, Š., Krobicki, M., Pruner, P., Reháková, D., Schnabl, P., Stoykova, K. & Wierzbowski, H., 2019. Integrated stratigraphy and palaeoenvironmental interpretation of the Upper Kimmeridgian to Lower Berriasian pelagic sequences of the Velykyi Kamianets section (Pieniny Klippen Belt, Ukraine). *Palaeogeography, Palaeoclimatology, Palaeoecology*, 532: 109216.

Grabowski, J., Haas, J., Stoykova, K., Wierzbowski, H. & Brański, P., 2017. Environmental changes around the Jurassic/Cretaceous transition: new nannofossil, chemostratigraphic and stable isotope data from the Lókút section (Transdanubian Range, Hungary). *Sedimentary Geology*, 360: 54–72.

Ivanova, D. & Kietzmann, D., 2017. Calcareous dinoflagellate cysts from the Tithonian – Valanginian Vaca Muerta Formation in the southern Mendoza area of the Neuquén Basin, Argentina. *Journal of South American Earth Sciences*, 77: 150–169.

Iwańczuk, J., Iwanow, A. & Wierzbowski, A., 2013. Lower Jurassic to lower Middle Jurassic succession at Kopy Sołtysie and Płaczliwa Skała in the eastern Tatra Mts (Western Carpathians) of Poland and Slovakia: stratigraphy, facies and ammonites. *Volumina Jurassica*, 11: 19–58.

Jach, R., 2007. *Bositra* limestones – a step towards radiolarites: case study from the Tatra Mountains. *Annales Societatis Geologorum Poloniae*, 77: 161–170.

Jach, R., 2021. Addendum to the chemostratigraphy of the uppermost Callovian–middle Oxfordian interval of the Tethyan Fatricum domain (Tatra Mts, Krížna Nappe, southern Poland). *Annales Societatis Geologorum Poloniae*, 91: 419–425.

Jach, R. & Reháková, D., 2019. Middle to Late Jurassic carbonate-biosiliceous sedimentation and palaeoenvironment in the Tethyan Fatricum Domain, Krížna Nappe, Tatra Mts, Western Carpathians. *Annales Societatis Geologorum Poloniae*, 89: 1–46.

Jach, R. & Starzec, K., 2003. Glaucony from the condensed Lower-Middle Jurassic deposits of the Krizna Unit, Western Tatra Mountains, Poland. *Annales Societatis Geologorum Poloniae,* 73: 183–192.

Jach, R., Djerić, N., Goričan, S. & Reháková, D., 2014. Integrated stratigraphy of the Middle–Upper Jurassic of the Krížna Nappe, Tatra Mountains. *Annales Societatis Geologorum Poloniae,* 84: 1–33.

Jenkyns, H. C., 1971a. Speculations on the genesis of crinoidal limestones in the Tethyan Jurasic. *Geologische Rundschau*, 60: 471–488.

Jenkyns, H. C., 1971b. The genesis of condensed sequences in the Tethyan Jurassic. *Lethaia*, 4: 327–352.

Jenkyns, H. C., 1974. Origin of red nodular limestones (Ammonitico Rosso, Knollenkalke) in the Mediterranean Jurassic: a diagenetic model. In: Hsü, K. J. & Jenkyns, H. C. (eds), *Pelagic Sediments: On Land and Under the Sea*. *International Associations of Sedimentologists*, *Special Publications*, 1: 249–271.

Jenkyns, H. C., Jones, C., Gröcke, D. R., Hesselbo, S. P. & Parkinson, D. N., 2002. Chemostratigraphy of the Jurassic System: applications, limitations and implications for palaeoceanography. *Journal of the Geological Society,* 159: 351–378.

Krobicki, M., Sidorczuk, M. & Wierzbowski, A., 2006a. Stop A8 – Jaworki-Homole Gorge (Fig. A12C). In: Wierzbowski, A., Aubrecht, R., Golonka, J., Gutowski, J., Krobicki, M., Matyja, B. A., Pieńkowski, G. & Uchman, A. (eds), *Jurassic of Poland and Adjacent Slovakian Carpathians, Field Trip Guidebook of 7th International Congress on the Jurassic System, Poland, Kraków, September, 6–18, 2006*. Polish Geological Institute, Warsaw, pp. 47–53.

Krobicki, M., Sidorczuk, M., Wierzbowski, A. & Uchman, A., 2006b. Stop A4 – Niedzica-Podmajerz (Fig. A12A) – Niedzica Succession (Aalenian–Tithonian). In: Wierzbowski, A., Aubrecht, R., Golonka, J., Gutowski, J., Krobicki, M., Matyja, B. A., Pieńkowski, G. & Uchman, A. (eds), *Jurassic of Poland and Adjacent Slovakian Carpathians, Field Trip Guidebook of 7th International Congress on the Jurassic System, Poland, Kraków, September, 6–18, 2006*. Polish Geological Institute, Warsaw, pp. 35–39.

Krobicki, M., Tyszka, J., Uchman, A. & Bąk, M., 2006c. Stop A2 – Flaki Range (Fig. A12B) – Branisko Succession (Bajocian–Oxfordian). In: Wierzbowski, A., Aubrecht, R., Golonka, J., Gutowski, J., Krobicki, M., Matyja, B. A., Pieńkowski, G. & Uchman, A. (eds), *Jurassic of Poland and Adjacent Slovakian Carpathians, Field Trip Guidebook of 7th International Congress on the Jurassic System, Poland, Kraków, September, 6–18, 2006*. Polish Geological Institute, Warsaw, pp. 29–35.

Krobicki, M. & Uchman, A., 2003. Trace fossils *Curvolithus* from the Middle Jurassic crinoidal limestones of the Pieniny Klippen Belt (Carpathians, Poland). *Geologica Carpathica,* 54: 175–180.

Krobicki, M. & Wierzbowski, A., 2004. Stratigraphic position of the Bajocian crinoidal limestones and their palaeogeographic significance in evolution of the Pieniny Klippen Basin. *Volumina Jurassica*, 2: 69–82. [In Polish, with English summary.]

Krobicki, M. & Wierzbowski, A., 2009. Środkowojurajskie (bajos–baton) wapienie bulaste sukcesji czertezickiej pienińskiego basenu skałkowego Polski i ich znaczenie paleogeograficzne – fakty i kontrowersje. *Przegląd Geologiczny*, 57: 600–606. [In Polish.]

Kwiatkowski, S., 1981. Sedimentation and diagenesis of the Niedzica Succession radiolarites in the Pieniny Klippen-Belt, Poland. *Annales Societatis Geologorum Poloniae*, 51: 45–61.

Lakova, I., 1993. Middle Tithonian to Berriasian praecalpionellid and calpionellid zonation of the western Balkanides. *Geologica Balcanica*, 23: 3–22.

Lakova, I., Stoykova, K. & Ivanova, D., 1999. Calpionellid, nannofossil and calcareous dinocyst bioevents and integrated biochronology of the Tithonian to Valanginian in the Western Balkanides, Bulgaria. *Geologica Carpathica*, 50: 151–168.

Lakova, I., Tchoumatchenco, P., Ivanova, D. & Koleva-Rekalova, E., 2007. Callovian to Lower Cretaceous pelagic carbonates in the West Balkan Mountains (Komshtitsa and Barlya sections): integrated biostratigraphy and microfacies. *Geologica Balcanica*, 36: 81–89.

Ławrynowicz, A., 2000. *Biostratygrafia i wykształcenie mikrofacjalne górnojurajskich wapieni bulastych (formacja wapienia czorsztyńskiego) sukcesji niedzickiej pienińskiego pasa skałkowego Polski*. Unpublished MSc. Thesis, AGH University of Krakow, 64 pp. [In Polish.]

Lee, G. H., Park, S. C. & Kim, D. C., 2000. Fluctuations of the calcite compensation depth (CCD) in the East Sea (Sea of Japan). *Geo-Marine Letters*, 20: 20–26.

Leinfelder, R. R., Schmid, D. U., Nose, M. & Werner, W., 2002. Jurassic reef patterns: the expression of a changing globe. In: Kiessling, W., Flügel, E. & Golonka, J. (eds), *Phanerozoic Reef Patterns. SEPM Special Publications*, 72: 465–520.

Lewandowski, M., Krobicki, M., Matyja, B. A. & Wierzbowski, A., 2005. Palaeogeographic evolution of the Pieniny Klippen basin using stratigraphic and palaeomagnetic data from the Veliky Kamenets section (Carpathians, Ukraine). *Palaeogeography, Palaeoclimatology, Palaeoecology,* 216: 53–72.

Lodowski, D. G., Szives, O., Virág, A. & Grabowski, J., 2024. The latest Jurassic–earliest Cretaceous climate and oceanographic changes in the Western Tethys: The Transdanubian Range (Hungary) perspective. *Sedimentology*, 71: 1843–1872.

Łuczyński, P., 2002. Depositional evolution of the Middle Jurassic carbonate sediments in the High-Tatric succession, Tatra Mountains, Western Carpathians, Poland. *Acta Geologica Polonica*, 52: 365–378.

Łuczyński, P., 2021. Early and Middle Jurassic tectonically controlled deposition in the High-Tatric succession (Tatricum), Tatra Mountains, southern Poland: a review. *Geological Quarterly*, 65: 16.

Martire, L., 1996. Stratigraphy, facies and synsedimentary tectonics in the Jurassic Rosso Ammonitico Veronese (Altopiano di Asiago, NE Italy). *Facies*, 35: 209–236.

Matyszkiewicz, J., 1996. The significance of *Saccocoma*-calciturbidites for the analysis of the Polish epicontinental Late Jurassic Basin: An example from the Southern Cracow-Wieluń Upland (Poland). *Facies*, 34: 23–40.

Michalík, J., Reháková, D., Grabowski, J., Lintnerová, O., Svobodová, A., Schlögl, J., Sobień, K. & Schnabl, P., 2016. Stratigraphy, plankton communities, and magnetic proxies at

the Jurassic/Cretaceous boundary in the Pieniny Klippen Belt (Western Carpathians, Slovakia). *Geologica Carpathica*, 67: 303–328.

Milaniak, P., 2021. *Middle and Upper Jurassic limestones and radiolarites of the Niedzica-Podmajerz section, Pieniny*. Unpublished MSc. Thesis, Institute of Geological Sciences Jagiellonian University, 49 pp. [In Polish, with English abstract.]

Molina, J. M., Reolid, M. & Mattioli, E., 2018. Thin-shelled bivalve buildup of the lower Bajocian, South Iberian paleomargin: development of opportunists after oceanic perturbations. *Facies*, 64: 19.

Navarro, V., Molina, J. M. & Ruiz-Ortiz, P. A., 2009. Filament lumachelle on top of Middle Jurassic oolite limestones: event deposits marking the drowning of a Tethysian carbonate platform (Subbetic, southern Spain). *Facies*, 55: 89–102.

Navarro, V., Ruiz-Ortiz, P. A. & Molina, J. M., 2012. Birth and demise of a Middle Jurassic isolated shallow-marine carbonate platform on a tilted fault block: Example from the Southern Iberian continental palaeomargin. *Sedimentary Geology*, 269–270: 37–57.

Nowak, W., 1968. Stomiosphaerids of the Cieszyn Beds (Kimmeridgian–Hauterivian) in the Polish Cieszyn Silesia and their stratigraphic value. *Rocznik Polskiego Towarzystwa Geologicznego*, 38: 275–327. [In Polish, with English summary.]

Nowak, W., 1973. Znaczenie *Parastomiosphaera malmica* (Borza) dla korelacji utworów dolnego tytonu w Karpatach. *Kwartalnik Geologiczny*, 17: 648–650. [In Polish.]

Nowak, W., 1976. *Parastomiosphaera malmica* (Borza) from the Polish Carpathians and their stratigraphical value for lower Tithonian deposits. *Rocznik Polskiego Towarzystwa Geologicznego*, 46: 89–134.

Ogg, J. G., Robertson, A. H. F. & Jansa, L. F., 1983. Jurassic sedimentation history of site 534 (western North Atlantic) and of the Atlantic-Tethys Seaway. In: Sheridan, R. E. & Gradstein, F. M. (eds), *Initial Reports of the Deep Sea Drilling Project*, 76: 829–884.

Olszewska, B., 2010. Microfossils of the Upper Jurassic–Lower Cretaceous formations of the Lublin Upland (SE Poland) based on thin section studies. *Polish Geological Institute Special Papers*, 26: 1–56.

Padden, M., Weissert, H., Funk, H., Schneider, S. & Gansner, C., 2002. Late Jurassic lithological evolution and carbon-isotope stratigraphy of the western Tethys. *Eclogae Geologicae Helvetiae*, 95: 333–346.

Pellenard, P., Tramoy, R., Pucéat, E., Huret, E., Martinez, M., Bruneau, L. & Thierry, J., 2014. Carbon cycle and sea-water palaeotemperature evolution at the Middle–Late Jurassic transition, eastern Paris Basin (France). *Marine and Petroleum Geology*, 53: 30–43.

Piuz, A. D., 2008. Microfaunistic associations of the Bajocian echinodermic shelf in the Jura Mountains and Burgundy: Paleoenvironmental implications. *Archives des Sciences*, 61: 120–128.

Price, G. D., Főzy, I. & Pálfy, J., 2016. Carbon cycle through the Jurassic–Cretaceous boundary: A new global $\delta^{13}C$ stack. *Palaeogeography, Palaeoclimatology, Palaeoecology*, 451: 46–61.

Rais, P., Louise-Schmid, B., Bernasconi, S. M. & Weissert, H., 2007. Palaeoceanographic and palaeoclimatic reorganization around the Middle–Late Jurassic transition. *Palaeogeography, Palaeoclimatology, Palaeoecology*, 251: 527–546.

Ramajo, J. & Aurell, M., 2008. Long-term Callovian–Oxfordian sea-level changes and sedimentation in the Iberian carbonate platform (Jurassic, Spain): possible eustatic implications. *Basin Research*, 20: 163–184.

Rao, V. P., Hegner, E., Naqvi, S. W. A., Kessarkar, P. M., Ahmad, S. M. & Raju, D. S., 2008. Miocene phosphorites from the Murray Ridge, northwestern Arabian Sea. *Palaeogeography, Palaeoclimatology, Palaeoecology*, 260: 347–358.

Rea, D. K. & Lyle, M. W., 2005. Paleogene calcite compensation depth in the eastern subtropical Pacific: Answers and questions, *Paleoceanography*, 20: PA1012.

Reháková, D., 2000a. Calcareous dinoflagellate and calpionellid bioevents versus sea-level fluctuations recorded in the West-Carpathian (Late Jurassic/Early Cretaceous) pelagic environments. *Geologica Carpathica*, 51: 229–243.

Reháková, D., 2000b. Evolution and distribution of the Late Jurassic and Early Cretaceous calcareous dinoflagellates recorded in the Western Carpathian pelagic carbonate facies. *Mineralia Slovaca,* 32: 79–88.

Reháková, D., Matyja, B. A., Wierzbowski, A., Schlögl, J., Krobicki, M. & Barski, M., 2011. Stratigraphy and microfacies of the Jurassic and lowermost Cretaceous of the Veliky Kamenets section (Pieniny Klippen Belt, Carpathians, Western Ukraine). *Volumina Jurassica*, 9: 61–104.

Reolid, M., Rivas, P. & Rodríguez-Tovar, F. J., 2015. Toarcian Ammonitico Rosso facies from South Iberian Paleomargin (Betic Cordillera, southern Spain): Paleoenvironmental reconstruction. *Facies*, 61: 22. [26 pp.]

Santantonio, M., 1993. Facies associations and evolution of pelagic carbonate platform/basin systems: examples from the Italian Jurassic. *Sedimentology*, 40: 1039–1067.

Thierry, J. & Barrier, E., 2000. Map 9. Middle Callovian (157–155 Ma). In: Dercourt, J., Gaetani, M., Vrielynck, B., Barrier, E., Biju-Duval, B., Brunet, M. F., Cadet, J. P., Crasquin, S. & Sandulescu, M. (eds), *Atlas Peri-Tethys. Palaeogeographical Maps*. Peri-Tethys Programme, Paris.

Tomašových, A., Schlögl, J., Michalík, J. & Donovalová, L., 2020. Noncondensed shell beds in hiatal successions: instantaneous cementation associated with nutrientrich bottom currents and high bivalve production. *Italian Journal of Geosciences*, 139: 76–97.

Tucker, M. E., 1974. Sedimentology of Palaeozoic pelagic limestones: the Devonian Griotte (southern France) and Cephalopodenkalk (Germany). In: Hsü, K. J. & Jenkyns, H. C. (eds), *Pelagic Sediments: On Land and Under the Sea*. *International Associations of Sedimentologists*, *Special Publications*, 1: 71–92.

Vörös, A., 2012. Episodic sedimentation on a peri-Tethyan ridge through the Middle–Late Jurassic transition (Villány Mountains, southern Hungary). *Facies*, 58: 415–443.

Weissert, H. & Channell, J. E. T., 1989. Tethyan carbonate carbon isotope stratigraphy across the Jurassic-Cretaceous boundary: an indicator of decelerated carbon cycling. *Paleoceanography*, 4: 483–494.

Weissert, H., Lini, A., Föllmi, K. B. & Kuhn, O., 1998. Correlation of Early Cretaceous carbon isotope stratigraphy and platform drowning events: a possible link? *Palaeogeography, Palaeoclimatology, Palaeoecology*, 137: 189–203

Weissert, H. & Mohr, H., 1996. Late Jurassic climate and its impact on carbon cycling. *Palaeogeography, Palaeoclimatology, Palaeoecology*, 122: 27–43.

Widz, D., 1991. Les radiolaires du Jurassique supérieur des radiolarites de la zone des Klippes de Pieniny (Carpathes Occidentales, Pologne). *Revue de Micropaléontologie, Paris*, 34: 231–260.

Wierzbowski, A., Jaworska, M. & Krobicki, M., 1999. Jurassic (Upper Bajocian-lowest Oxfordian) ammonitico rosso facies in the Pieniny Klippen Belt, Carpathians, Poland: its, fauna, age, microfacies and sedimentary environment. *Studia Geologica Polonica*, 115: 7–74.

Wierzbowski, A., Krobicki, M. & Matyja, B. A., 2012. The stratigraphy and palaeogeographic position of the Jurassic successions of the Priborzhavske-Perechin Zone in the Pieniny Klippen Belt in the Transcarpathian Ukraine. *Volumina Jurassica*, 10: 25–60.

Wierzbowski, A., Wierzbowski, H., Segit, T. & Krobicki, M., 2021. Jurassic evolution and the structure of the central part of the Pieniny Klippen Belt (Carpathians) in Poland – new insight from the Czertezik Succession type area. *Volumina Jurassica*, 19: 21–60.

Wierzbowski, H., 2015. Seawater temperatures and carbon isotope variations in central European basins at the Middle–Late Jurassic transition (Late Callovian–Early Kimmeridgian). *Palaeogeography, Palaeoclimatology, Palaeoecology*, 440: 506–523.

Wierzbowski, H., Wierzbowski, A. & Pańczyk, M., 2012. Tuffite layer in the Niedzica Limestone Formation (Late Bathonian–Callovian), Pieniny Klippen Belt, Poland: preliminary results of petrographic analyses. In: Józsa Š., Reháková D. & Vojtko R. (eds): *Environmental, Structural and Stratigraphical Evolution of the Western Carpathians 8th Conference 2012, Abstract Book, 6th–7th December, Bratislava*. Bratislava, p. 55.

Wignall, P. B., 1993. Distinguishing between oxygen and substrate control in fossil benthic assemblages. *Journal of the Geological Society,* 150: 193–196.

Wilson, J. L., 1975. *Carbonate Facies in Geologic History*. Springer-Verlag, Berlin, Heidelberg, 471 pp.

Winterer, E. L. & Bosellini, A., 1981. Subsidence and sedimentation on Jurassic passive continental margin Southern Alps, Italy. *American Association of Petroleum Geologists Bulletin*, 65: 394–421.